buildings

MDPI

Review

Comprehensive Review of Binder Matrices in 3D Printing Construction: Rheological Perspectives

Yeşim Tarhan [1,*], İsmail Hakkı Tarhan [2] and Remzi Şahin [3]

[1] Technical Sciences Vocational School, Ardahan University, Ardahan 75000, Türkiye
[2] Department of Civil Engineering, Faculty of Engineering and Architecture, Tokat Gaziosmanpaşa University, Tokat 60150, Türkiye; ismailhakki.tarhan@gop.edu.tr
[3] Department of Civil Engineering, Atatürk University, Erzurum 25030, Türkiye; rsahin@atauni.edu.tr
* Correspondence: yesimtarhan@ardahan.edu.tr; Tel.: +90-5388630139

Abstract: Three-dimensional printing technology is transforming the construction industry, which is increasingly turning to advanced materials and techniques to meet environmental and economic challenges. This comprehensive literature review evaluated various binder materials, including cement, geopolymers, earthen materials, supplementary cementitious materials, polymers, and biopolymers, with a focus on their environmental impacts and rheological properties. The study revealed an increasing interest in cementitious binders, which deliver essential structural strength and exhibit a wide range of yield stress values (15 to 6500 Pa), influenced by binder type and supplementary materials such as nanoclay. However, the significant CO_2 emissions associated with cement pose major sustainability challenges. As a sustainable alternative, geopolymers demonstrate lower yield stress values (800 to 3000 Pa) while ensuring adequate buildability for vertical printing and reducing environmental impact. These findings underscore the need to adopt sustainable binder matrices to align 3D printing construction practices with global sustainability goals.

Keywords: 3D printing concrete; cementitious materials; earth-based binder; geopolymer; concrete; sustainability

check for updates

Academic Editor: Bo-Tao Huang

Received: 22 November 2024
Revised: 16 December 2024
Accepted: 25 December 2024
Published: 29 December 2024

Citation: Tarhan, Y.; Tarhan, İ.H.; Şahin, R. Comprehensive Review of Binder Matrices in 3D Printing Construction: Rheological Perspectives. *Buildings* **2025**, *15*, 75. https://doi.org/10.3390/buildings15010075

Copyright: © 2024 by the authors. Licensee MDPI, Basel, Switzerland. This article is an open access article distributed under the terms and conditions of the Creative Commons Attribution (CC BY) license (https://creativecommons.org/licenses/by/4.0/).

1. Introduction

One of the most consumed commercial materials globally is concrete, derived from the combination of aggregate, water, cement, and some additives in precise quantities [1,2]. To address the challenges and demands related to the carbon footprint and economic pressures of the construction industry, practitioners and researchers have concentrated on developing innovative materials and new production techniques. Three-dimensional (3D) Printing Construction (3DPC) is an innovative construction process based on additive manufacturing (AM) technology. This method, which is promising in recent developments, has attracted worldwide interest. During the last decade, 3DPC technologies have emerged as transformative technologies, offering fast and cost-effective production of complex geometries in the structural design process and significant advances in the transition to automation in the construction industry [3–5].

Although the construction industry is still at the beginning of automation and digitalisation steps within the scope of Industry 4.0, which aims to digitalise various sectors, it is actively pursuing advancements through ongoing research endeavours to align itself with this industrial transformation [6]. AM, introduced with the development of Industry 4.0, is one of the newest technological forms in the construction sector [7]. To enable physical-to-digital transformations, this technology combines sensors and controllers, cognitive

and high-performance computing, augmented reality, additive manufacturing, advanced materials, autonomous robotics, digital design, and simulation systems [8]. The AM sector continues to evolve with new techniques, materials, and 3D printers. Three-dimensional printing technology is advancing toward the capabilities of creating 4D printed structures by responding to external influences like temperature, light, moisture, or stimuli [9,10]. The transformative effect of 3D printing on construction must be balanced, effectively minimizing key project determinants, such as construction time, material usage, budget, and overall project duration [11]. First pioneered by Charles (Chuck) Hull in 1984, this technology uses numerical data to produce three-dimensional objects [12]. The 3DPC technology reduces material consumption [13], introduces lightweight properties to products [14], and allows the creation of multifunctional components [15].

Despite its potential, 3DPC technology faces challenges such as insufficient stiffness and strength of printed materials [16], cold joints from layering [17], limited design size due to printer chamber volume [18], and the need for support during printing for stability [19]. Additional issues include complex mix design [20], rough surface appearance [21], and high printer costs [22]. Three-dimensional printing in construction necessitates collaboration between materials science, computing, and computer-aided design experts [23]. While these challenges are broadly categorised as material, printer, software, computational, architectural and design, construction management, regulatory, and stakeholder issues, material printability, constructability, and open time are the most frequently cited concerns in the literature. Selecting appropriate binders is critical [24] due to the complexities of producing 3D printable mixes that meet these criteria.

This study systematically evaluates binder materials used in 3D printing construction, emphasizing their unique rheological characteristics, advantages, limitations, and sustainability. The literature review was conducted using the Scopus database, chosen for its extensive coverage in engineering and technology, ensuring access to publications aligned with the study's objectives. A precise keyword strategy was employed, including terms like "3D printing", "geopolymers", and "sustainable binders", while excluding unrelated terms such as "ceramics". Boolean operators and inclusion/exclusion criteria were refined in the search results. Publications from 2010–2024 were reviewed to capture the accelerated advancements in 3D printing construction during this period. Cement, earth, geopolymer, and biopolymer-based binders were comprehensively evaluated for their rheological properties, mechanical performance, and environmental impacts. The filtered publications were categorized into thematic areas such as material properties, rheology, and sustainability, enabling an in-depth analysis and synthesis of critical insights. By consolidating current research and identifying knowledge gaps, this review aims to guide the development of more efficient and sustainable practices in 3D printing for construction.

2. Review Methodology

The literature review, focusing on titles, abstracts, and keywords, was conducted using the Scopus database due to its extensive coverage in engineering and technology, providing access to critical publications aligned with the research objectives. The selected keywords were "3D printing", "3D-printed", "additive manufacturing", "concrete", "cement", "geopolymer", "earth", "lime", "supplementary cementitious materials", and "SCMs" to accurately achieve the intended review focus. Moreover, the terms "ceramic" and "bioceramic" were excluded, and Boolean operators were used, as detailed in Table 1, to obtain a comprehensive view of the research. The review focused on publications written in English between 2010 and 2024, a period when technology has experienced accelerated development.

Table 1. Literature review terminologies.

3D Printable Bases	Search Expression
Cementitious	3D printing OR 3D-printed OR Additive manufacturing AND (concrete OR cement) AND NOT ceramic AND NOT bioceramic
Sustainable	3D printing OR 3D-printed OR Additive manufacturing AND (geopolymer OR earth OR lime) AND NOT ceramic AND NOT bioceramic
Sustainable cementitious	3D printing OR 3D-printed OR Additive manufacturing AND (concrete OR cement) AND supplementary cementitious materials OR SCMs OR fly ash OR slag OR silica fume OR rice husk AND NOT ceramic AND NOT bioceramic

One of the two publishers contributing significantly to 3D printing research is MDPI, where this study is also presented. With around 2400 papers published in the last three years, it represents 25% of the output from the top ten sources, which include both journals and conference proceedings (see Figure 1a). The search for 3DPC yielded a total of 5099 unique publications after removing duplicates from overlapping keyword searches. Of these, 60.7% were focused on engineering and materials science subject areas (see Figure 1b). Most publications focused on cementitious mixtures, comprising 69.0% of the total (see Figure 1c). The distribution of publications by year (Figure 1d) clearly shows the growing interest in cementitious mixtures. However, despite the importance of sustainable cementitious mixtures, interest is developing routinely, and it is clear that if current trends continue, sustainability will be neglected.

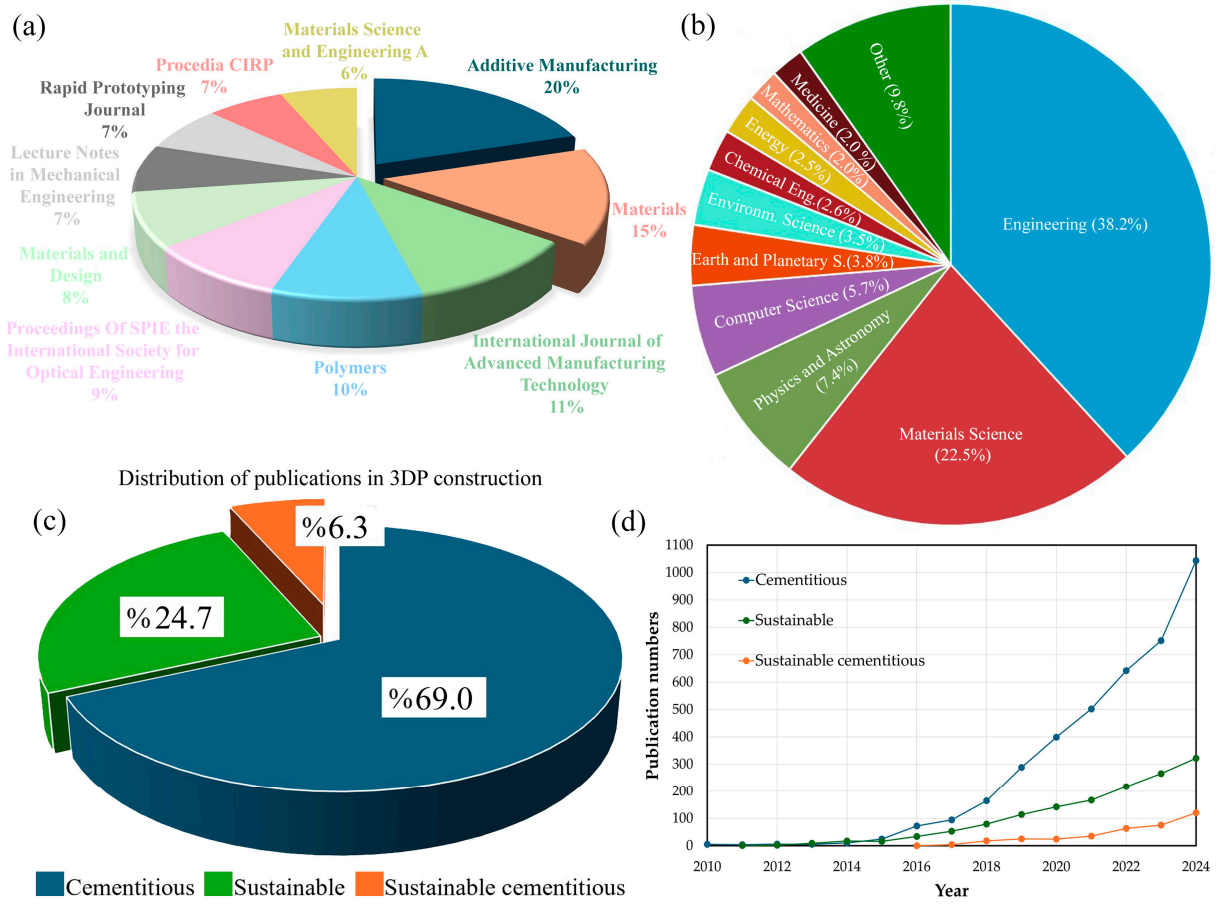


Figure 1. (**a**) Distribution of publications on 3D printing among journals, (**b**) publication distribution by field, (**c**) publication distribution in 3DPC field considering base material, (**d**) growing publication interest depending on base material in 3DPC field over the years.

According to Figure 2a, which ranks countries by the number of publications on 3D printing and 3DPC, China, Germany, Australia, France, Russia, Singapore, the Netherlands, Switzerland, and Belgium focus more on using 3D printing in construction than in other fields. The top five countries with the most publications on 3DPC are China, the United States, Germany, Australia, and the United Kingdom. Figure 2b also shows the distribution of publication numbers using a colour scale on the world map.

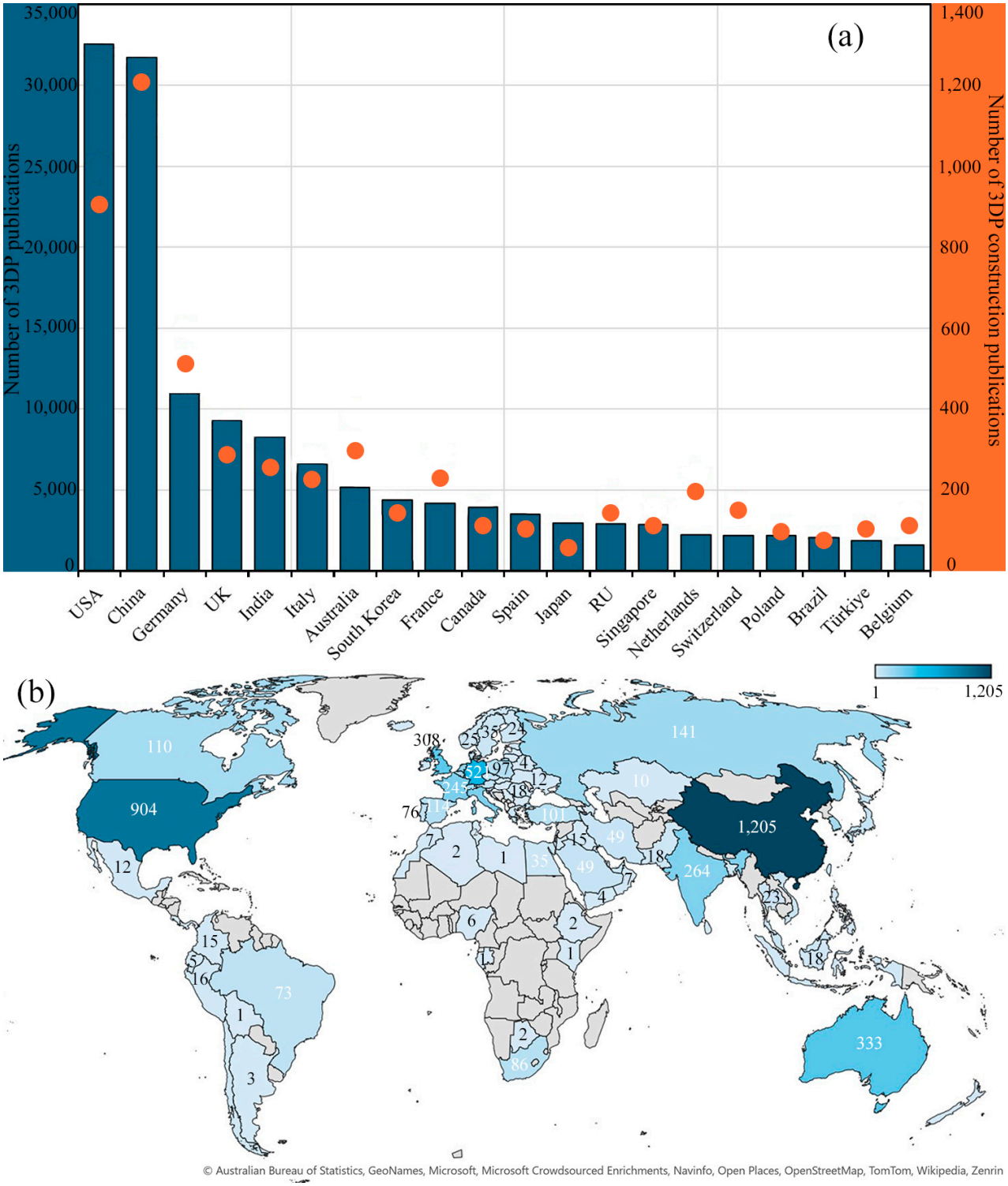


Figure 2. (**a**) Publication numbers of countries on 3DP and 3DPC, (**b**) publication distribution of countries on the world map (3DPC).

3. Enhancing the Benefits of 3D Printing in Construction

Digital concrete production is an up-and-coming research field, enabling the construction of complex architectures with freedom from formwork, accelerated construction with increased automation, and cost-effective production with productivity [25]. Three-dimensional printing in construction offers substantial economic and environmental advantages over traditional methods by eliminating mold and labor costs, reducing construction time by up to 95%, lowering CO_2 emissions by approximately 32%, and minimizing waste generation [26–31]. However, high initial investment, maintenance, and operational costs, scalability challenges, and the energy consumption of 3D printers (especially large-scale models), along with complex mixture properties requiring expensive chemical additives, limited suitable materials, and predominantly higher binder content, can potentially increase both costs and environmental harm [26,30,32].

The construction industry's sustainable development goals include building robust structures, fostering inclusive and sustainable urban environments, and enhancing resource efficiency. To improve the sustainability of concrete, it is essential to reduce cement content and water usage, preserve natural aggregate resources, and, thus, reduce CO_2 emissions while improving mechanical and durability performance. Three-dimensional printing concrete technology offers opportunities to realize these goals [33–36].

The AM process necessitates materials possessing both pumpability (extrudability) and properties conducive to layer-by-layer (buildability) construction [37–39]. These properties are critical for the successful application of 3DCP technologies, as they ensure the material can be pumped through a nozzle, extruded in a manner, and maintain shape once deposited [40,41]. For large-scale AM applications, the ink (printable concrete) must be formulated to ensure smooth extrusion through a nozzle while providing adequate support for the structural components of the subsequent layers. The capacity of concrete to flow unaltered through a concrete pump, transmission pipe, and spray nozzle is defined as its extrudability. The height of the printed structure and the concrete layer's ability to solidify and carry subsequent layers determine buildability [42–44]. Three-dimensional printing concrete's rheological properties, including shear strength (yield stress) and viscosity, are crucial for its printability. The composition of ingredients significantly impacts the material's rheological behavior [45,46]. Thixotropy, a time-dependent property, is crucial in 3D printing research as it ensures suitable flowability for extrusion and printability. The mixture must possess a suitable thixotropic consistency and prompt stiffening response for improved buildability. Balancing printability and material strength in the hardened state requires careful adjustment of water content and plasticity. Three-dimensional printing mixtures must consist of a precise blend of chemical admixtures to boost workability and comprise fine particles for effortless nozzle flow, necessitating a meticulous selection of materials [37,44,47]. The workability, setting time, and mechanical properties of the printed structures can be significantly influenced by various additives, including cellulose microfibers, viscosity-modifying agents (VMA), and mineral additives [48,49]. The binder's unique characteristics indeed necessitate specific qualifications for 3D printable mixes. These mixes utilize a variety of binders, including cement, geopolymers, earth–clay binders, and sustainable cementitious materials, each with distinct properties affecting the printability, mechanical performance, and sustainability of the final product [49,50].

3.1. Cement Matrix Inks

Three-dimensional printable concrete is a new-generation construction material consisting of cement, water, aggregates (predominantly fine), minerals [51–53], and chemical admixtures [51,54,55]. It can also include fibers (to reduce shrinkage and crack formation [56–59]) and some types of clay minerals, contributing to improved shape stability and

print quality [20,54,60,61]. Cement is recognized as a crucial binding agent in 3D-printed concrete, and research is currently focused on improving the performance of 3D-printed structures. Studies have considered different cement-based materials and their combinations to evaluate how they affect mechanical properties and durability when utilized in 3DCP [62,63]. Research is also focused on various cement-based materials and their combinations to evaluate their impact on the mechanical properties and durability of 3D-printed concrete [41,42,50,64–70].

Interestingly, while cement is essential for the structural integrity of 3D-printed concrete, its use also presents environmental concerns due to greenhouse gas emissions [71,72]. The contradiction stems from the necessity to balance the structural demands of concrete with the environmental imperative to reduce greenhouse gas emissions. Cement is crucial for concrete's mechanical properties, yet its production is energy-intensive and a major source of CO_2 emissions [73]. Three-dimensional printed concrete requires a higher cement content for adequate extrudability, strength, and buildability compared to conventional concrete [74].

As global greenhouse gas (GHG) emissions continue to rise, the resulting impacts of climate change are becoming more severe and pose a significant threat to the world. The construction sector is a particularly important part of this threat, accounting for 37% of global CO_2 emissions by 2021 [75]. The production of cement unequivocally poses a significant threat to the climate, primarily due to its high-energy usage during clinker transformation into cement and the ensuing intense CO_2 emissions during calcination [76]. Seven percent or more of yearly anthropogenic greenhouse gas (GHG) emissions originate from cement production, impeding the goal of reaching net-zero emissions by 2050 [77]. However, cement manufacturing remains one of the most demanding industries for decarbonisation, and, depending on the increasing population, the demand for cement is increasing day by day [78].

Decarbonisation strategies include reducing traditional cement production, substituting clinkers, switching fuels, adopting novel technologies, and implementing carbon pricing [79,80]. Cement production contributes to approximately 85% of the total CO_2 emissions from concrete (250 kg CO_2/m^3) [81]. Consequently, developing new types of cement with low or very low carbon emissions has become a significant area of research and investigation. Examples of novel cements are as follows: i. Magnesium silicates cement, rather than limestone cement [82,83], ii. Belitic Calcium SulfoAluminate (BCSA) cement [84], iii. Cement is produced through the rapid calcination of dolomite rock in superheated steam, coupled with carbon dioxide capture [85], iv. Geopolymer cement is created using waste materials from the power industry, such as fly ash and ground granulated blast furnace slag (GGBS) [86,87].

Three-dimensional-printed concrete technology, characterised by its use of small nozzle diameters and absence of coarse aggregates, initially appears economically sustainable. However, the reliance on increased cement content may jeopardise its sustainability. While 3D printing techniques demonstrate superiority in reducing environmental impact compared to traditional methods, efforts to mitigate CO_2 emissions should prioritise minimizing cement usage for a truly sustainable approach.

Calcium sulfoaluminate cement (CSA), a low-CO_2 alternative, has gained popularity as a promising binder alternative to Portland cement [88,89], while other alternatives like limestone calcined clay cement (LC_3) and reactive magnesium oxide systems are also being explored [90], as well as reactive magnesium oxide systems [91,92]. CSA is recognized for its lower carbon footprint compared to ordinary Portland cement (OPC) [93,94], making it an attractive alternative for sustainable construction practices, including 3D printing of concrete [95]. CSA's early-age expansion can be beneficial in countering shrinkage cracking,

a significant advantage for 3D-printed structures that may be prone to such issues due to their layer-by-layer construction [96]. Mohan et al. [97] explored the viability of CSA cement as a binder for 3D printable concrete. The early-age hydration of CSA cement mixtures was studied to determine the effectiveness of borax and gluconate as retarders. Despite a similar lubricating layer behavior, the CSA mixture necessitated a higher pumping pressure due to its superior plastic viscosity compared to the CSA and PC mixtures. Although CSA improves mechanical properties and reduces shrinkage deformation in concrete, it raises the risk of carbonation and corrosion in steel rebars [98]. Jianchao et al. [99] examined the properties of cementitious mortars made with OPC and sulphoaluminate cement (SAC). SAC sets faster and has greater early strength than OPC. Three-dimensional printing mortar is best suited to SAC material due to its quick initial setting time. The lower layers must be strong enough to carry the weight of the upper layers.

The rheological properties of 3D printable cement-based mixtures, including yield stress, shear stress, viscosity, and thixotropic index, are essential for understanding material behavior during printing. A summary of the literature on the characterization of these properties, along with material compositions, component variations, testing equipment, material models, and key findings, is presented in Table 2.

Table 2. Rheological properties of cement-based 3D printable mixtures.

Name	Materials	Material Parameters	Test Equipments/Models	Rheological Properties	Key Findings
Zhang et al. [54]	Type II 52.5 Portland cement (PC), nanoclay, silica fume (SF), fine aggregate, retarder, thickening agent, superplasticizer (SP)	-Water/binder: 0.35, -Nanoclay content: 0–2% cement replacement, -SF content: 0–2% cement replacement	-Brookfield rheometer with vane spindle -Bingham model for rheological analysis	-Yield stress range: 15–200 Pa, -Viscosity range: 3.5–5 Pa.s -Thixotropy range: 4000–16,000 Pa/s	The addition of nanoclay and SF greatly enhanced buildability, thixotropy, and green strength in 3D printable concrete. The optimized mixture containing both showed the best overall performance in rheology and buildability.
Xu et al. [100]	Ordinary portland cement (OPC), sulphoaluminate cement (SAC), fly ash (FA), ground granulated blast furnace slag (GGBS), sand, water reducing agent, rubber powder, cellulose ether, defoamer, accelerator, early strength agent.	-FA content: 0–40% replacement of OPC, -GGBS content: 0–40% replacement of OPC -Water-binder ratio: 0.32	-Mars40 rheometer -Slump test	For Optimal mixture (20% FA): -Slump: 42 mm, -Expansion: 185 mm, -Apparent viscosity: 1.5–4.5 Pa.s, -Shear stress: 38–58 Pa	The addition of 20% FA resulted in optimal rheological properties for 3D printing, with the lowest apparent viscosity and shear stress, and the best extrusion and buildability performance. FA and GGBS can improve rheological properties.
Rubio et al. [101]	Cement, FA, SF, sand, Polypropylene (PP) fibers, SP, viscosity modifying agents (VMA) (diutan gum, nanoclay)	-Water/binder: 0.50, Binder/sand: 0.50, PP fibers: 0.2–0.6% by volume, -SP: 0.275–0.55% of binder, -VMA1 (diutan gum): 0.05% of binder, -VMA2 (nanoclay): 0.10% of binder	-Flow table -Penetration -Cylinder slump -Haake VT550 vane viscometer -Modified Bingham model	-Yield stress: 0–1079 Pa -Slump flow: 140–280 mm -Penetration: 19–40 mm	FA and SF increased yield stress and stability in 3D printing. PP fibers improved cohesiveness but hindered extrusion. VMAs enhanced stability but reduced workability.

Table 2. *Cont.*

Name	Materials	Material Parameters	Test Equipments/Models	Rheological Properties	Key Findings
Yuan et al. [102]	Cement, sand, SP, attapulgite (AG) clay, SAC, sodium gluconate (SG)	-w/c: 0.35, -s/b: 1.5, -AG clay: 0–1% of binder, -SAC: 0–10% PC, SG: 0–0.0008% of binder	-Coaxial cylinder rotary rheometer -Bingham model, -Penetration resistance test	-Static yield stress: 500–4000 Pa, -Dynamic yield stress: 250–580 Pa, -Plastic viscosity: 5.5–8.5 Pa.s, -Penetration resistance: 0–35 kPa (over 10 h)	AG clay enhanced thixotropy, while SAC accelerated structural buildup. Optimal printing intervals varied between 2–10 min depending on the mix. Penetration resistance showed strong correlation with static yield stress growth.
Kruger et al. [103]	Cement, FA, SF, sand, SP	-Water/cement ratio: 0.45	-Germann ICAR Plus rheometer -Stress growth test	-Static yield stress: 6020 Pa -Dynamic yield stress: 692 Pa	An analytical shape retention model for 3D-printed concrete, which uses only rheological properties to predict the maximum stable filament layer height, is developed. This model ensures no plastic yielding occurs under self-weight, which is critical for maintaining shape retention and buildability.
Kruger et al. [104]	Cement, FA, SF, sand, SP, VMA, nano-silica	-Water/cement: 0.45, -SP: −15% to +15% of reference dosage, -Nano-silica: 0–3% by mass of cement	-Germann ICAR Plus Rheometer -Stress growth test	-Static yield stress: 2108–6483 Pa, -Dynamic yield stress: 420–2803 Pa, -Reflocculation rate (Rthix): 1.36–8.00 Pa/s, -Structuration rate (Athix): 0.61–1.17 Pa/s	A novel bi-linear thixotropy model was developed for 3D printable concrete, distinguishing between Rthix and structuration Athix rates. Rthix was found to be a better indicator of thixotropic behavior for 3D printing than Athix.

Table 2. *Cont.*

Name	Materials	Material Parameters	Test Equipments/Models	Rheological Properties	Key Findings
Lee et al. [105]	OPC, ISO standard sand, water, high water reducing agent	-Water/binder: 0.30, -High water reducing agent: 0.3% -Sand weight: 0.40–0.55 (by total weight)	-Anton Paar rheometer -Hysteresis loop measurements -Buildup ratio measurements	-Hysteresis loop area: 5647–49,242 Pa/s -Buildup ratio: 0.66–0.81	A close correlation was found between thixotropic behavior (measured by hysteresis loop area and buildup ratio) and 3D printing buildability. The resting time required for stable buildability could be predicted through analysis of thixotropic behavior.
Weng et al. [106]	OPC, SF, FA, silica sand, natural river sand, water, SP	-Water/binder: 0.30, -Sand/binder: 0.50, -Sand gradation: Varied based on Fuller Thompson theory, uniform gradation, gap gradation	-Viskomat XL rheometer -Bingham plastic model -Mini-slump test	-Static yield stress: 1874–3350 Pa, -Dynamic yield stress: 208.4–492.7 Pa, -Plastic viscosity: 16.65–33.31 Pa.s	A mixture based on Fuller–Thompson showed the best buildability, with high yield stress, low plastic viscosity, and stable printing of up to 40 layers.
Zhang et al. [107]	PC, SF, nano-silica, micro-AG clay, sand, SP	-SP dosage: 0.8–1% by mass of binder, -Water-to-binder ratio: 0.215–0.340, -Sand-to-binder ratio: 1.41–2.24, -Sand maximum particle size: 1.18–4.75 mm	-Mini-slump test for paste flowability -Brookfield rheometer for yield stress, -Cylinder stability test for buildability assessment	-Yield stress: 2300–2730 Pa	A linear relationship was identified between cement paste flowability and optimal sand content for printable mixes. Using this with the excess paste theory helps design 3D printable mixes with varying sand fineness, ensuring suitable rheology by adjusting sand content based on paste flowability.

Table 2. *Cont.*

Name	Materials	Material Parameters	Test Equipments/Models	Rheological Properties	Key Findings
Mohan et al. [97]	CSA cement, PC, limestone powder, sand, SP, VMA, retarders (borax, sodium gluconate)	-Water-to-binder: 0.35, -Aggregate-to-binder: 1.5, -VMA dosage: 0.1% by weight of binder, -Retarder dosage: 0.5% by weight of binder, -Limestone powder substitution: 0–30% replacement of CSA	-Anton Paar MCR 52 rheometer -Tribometer with smooth Couette geometry -Bingham model -Kaplan model for pumping pressure prediction	-Yield stress: 618–742 Pa, -Plastic viscosity: 22.3–62.1 Pa.s, -Lubricating layer yield stress: 241.7–269.7 Pa, -Lubricating layer viscous constant: 6830.2–7364.0 Pa.s/m	Borax can increase the open time of CSA mixtures without compromising early strength. CSA mixtures showed higher pumping pressures due to higher plastic viscosity. Limestone substitution reduced plastic viscosity and pumping pressures. CSA–limestone mixtures showed improved buildability compared to Portland cement mixtures.
Moeini et al. [108]	Cement paste (ternary blended cement containing PC, FA, SF), nanoclay (bentonite and halloysite), SP, quartz sand	-Water/binder: 0.35, by the mass of the binder: -Nanoclay content: 0–0.50% -SP content: 0–0.3%, -Sand/binder: 0.75–1.00	-Anton Paar MCR 302 rheometer with coaxial cylinders and parallel plate geometries -Mini-slump flow test (ASTM C1437) -Bingham model	For optimal paste mixture(H50HR3) -Static yield stress: 27 Pa (at t = 0), -Static yield stress: 140–1100 Pa, -Plastic viscosity (Pa. s) 1.7–4.0 Pa.s, -Dynamic yield stress (Pa) 58.3–76.2 Pa, -Thixotropy coefficient (Athix): 10.1–60 Pa/min,	Different rheometric methods provided insights into different aspects of material build-up. Static yield stress evolution was suitable for assessing sheared material behavior.

Table 2. *Cont.*

Name	Materials	Material Parameters	Test Equipments/Models	Rheological Properties	Key Findings
Qian and De Schutter [109]	PC, nanoclay (purified AG clay), polycarboxylate ether superplasticizer (PCE)	-Water/cement: 0.4 -Nanoclay content: 0–0.5% by mass of cement -PCE content: 0–0.2% by mass of cement	-Anton-Paar MCR 102 rheometer with coaxial cylinder geometry	-Range for mixtures: Dynamic yield stress: 2.5–27.5 mNm Thixotropic index: 1.1–3.3	Nanoclay increased thixotropy and dynamic yield stress at all PCE dosages. A half-percent of nanoclay maintained high thixotropy even at high PCE dosages. A nanoclay and PCE combination allows for the achievement of low dynamic yield stress yet high thixotropy, which is desirable for applications like 3D printing.
Tarhan and Sahin [20]	CEM I 52.5 R white cement, GGBS, calcined kaolin clay, silica sand, PP fibers, SP, VMA, cement hydration control agent, setting accelerator, air-entraining	-Water/binder: 0.35, -GGBS: 20% of cement weight, -PP: 0.2% of mixture volume, -Total aggregate: 1.24 binder amount, -Air-entraining admixture: 0–0.2% of binder	-Anton Paar RheolabQC rotational rheometer, -Bingham model for rheological analysis	-Yield stress range: 50–262 Pa, -Viscosity range: 24,606–47,697 mPa.s, -Thixotropy range: 18,288–25,877 Pa/s	Air-entraining admixture decreased yield stress and viscosity but interestingly increased thixotropy of 3D printable mortar mixes. The rheological properties were found suitable for 3D printing applications.
Bos et al. [64]	PC, FA, SF, sand, SP	Water/binder ratio: 0.45	-Schleibinger Viskomat XL rheometer -Bingham model for rheological analysis	-Static yield stress: 630–3180 Pa, -Dynamic yield stress range: 40–1450 Pa (initial values), -Thixotropy -(Rthix) range: 4.9 to 6.6 Pa/s, -Athix range: 0.6 to 3.1 Pa/s	Different test methods provided varying and sometimes conflicting results for material property development. Shear strength correlations required assuming high friction angles tied to Mohr–Coulomb failure.

Table 2. *Cont.*

Name	Materials	Material Parameters	Test Equipments/Models	Rheological Properties	Key Findings
Panda et al. [110]	OPC, FA, microsilica, sodium sulphate, sand, nanoclay (AG)	-Water/binder: 0.30, -Sand/binder: 0.83, -Time: 0–150 min after mixing, -Nanoclay content: 0–0.5% of binder	-Anton Paar MCR 102 rheometer	-Yield stress range: ~4000 Pa	Nanoclay enhanced early stiffness and green strength, improving buildability. A mathematical model was created to predict layer deformation during printing based on material properties and time.
Harbouz et al. [111]	Cement, sand, SP, VMA, supplementary cementitious materials (SCM) (FA, SF, limestone filler, kaolinite)	-Water-to-binder ratio: 0.28, -SP dosage: 0.3–1.2% by weight of cement, -VMA dosage: 0–1.5% by weight of cement, SCM types and combinations	-Discovery hybrid rheometer with vane-in-cup geometry	-Initial static yield stress: 100–500 Pa, -Athix: 4–15 Pa/min, -Rthix: 5–23 Pa/min, -Viscosity recovery rate (R): 0.4–0.95	The study proposed a new "WEB" (workability, extrudability, buildability) approach for assessing printability. Optimal printability was achieved with $0.006 < W < 0.015$, $E > 2.5$, and $B < 2$, where W, E, and B are indices derived from rheological parameters.
Zhang et al. [40]	Cement, sand, SP (HRWR), nanoclay, SF, thickening agent	-Water-to-cement: 0.35, -Sand-to-cement (S/C): 0.6 to 1.5	-Rheometer and Bingham Model	-Viscosity: 3.8–4.5 Pa.s, -Yield stress: 178.5–359.8 Pa, Thixotropy: <6284.5 Pa/s	The study identified an optimal S/C ratio range of 1.0–1.2 for 3D printing concrete, balancing pumpability, extrudability, and buildability.

Table 2. *Cont.*

Name	Materials	Material Parameters	Test Equipments/Models	Rheological Properties	Key Findings
Mohan et al. [112]	Cement (CEM I 52.5 N), GGBS, fine aggregate (max 2 mm), SP, VMA	-Water-to-binder: 0.35, -Aggregate-to-binder (a/b): 1.0 to 1.8, -SP dosage: adjusted to maintain flow value of 50–60%	-Anton Paar MCR-52 dynamic shear rheometer -Tribometer tests, -Krieger–Dougherty and Chateau–Ovarlez–Trung models for the analysis of the influence of aggregate content on the rheological behavior	-Plastic viscosity: 15.3–41.2 Pa·s -Yield stress: 627.6–828.4 Pa -Lubrication layer yield stress: 124.7–182.8 Pa -Lubrication layer viscous constant: 4399.5–5781.8 Pa.s/m	Increasing aggregate content significantly increased plastic viscosity and moderately increased yield stress and storage modulus of printable mixtures. The study demonstrated that rheological properties of both bulk concrete and lubrication layer influence on the pumping behavior of high-yield stress printable concretes.
Chen et al. [113]	CSA, hydroxypropyl methyl cellulose (HPMC), water reducing agent (WRA), sodium gluconate (SG), ultrafine quartz sand, bentonite	-Water-to-cement ratio: 0.35, -Bentonite content: 0–3% of cement mass	-Rotational rheometer (kinexus lab+, Malvern), -Bingham model	-Dynamic yield stress: 602.53–717.77 Pa, -Plastic viscosity: 2.37–2.97 Pa.s, -Static yield stress: 580–730 Pa, -Thixotropic parameter: 0.267–0.574	The addition of 2% bentonite achieved optimal 3D printability with plastic viscosity below 2.50 Pa·s and dynamic yield stress below 645.54 Pa. Bentonite improved structural stability and reduced deformation over time.
Long et al. [114]	OPC, FA, SF, microcrystalline cellulose (MCC), superplasticizer (HRWRA), lithium carbonate (accelerator), fine aggregate (max 1 mm)	-Water-to-binder ratio: 0.27–0.35, -MCC content: 0–1.5 wt% of binder	-RM 100 touch rheometer, -Bingham model	-Plastic viscosity: 7.41–12.71 Pa.s -Yield stress: 414.14–1201.24 Pa -Thixotropy: 64,220.14–173,463.26 Pa/s	The addition of 1 wt% MCC provided optimal rheological properties and buildability for 3D printing. Compared to the control mix, plastic viscosity and yield stress increased by 20.9% and 190.0%, respectively.

Table 2. *Cont.*

Name	Materials	Material Parameters	Test Equipments/Models	Rheological Properties	Key Findings
Tran et al. [115]	OPC, FA, SF, limestone powder, PP fiber, sand, SP	-Water-to-binder ratio (W/B): 0.22–0.30 -Sand-to-binder ratio (S/B): 0.58–0.94, -PP fiber content: 0–5.4 kg/m^3, -SP dosage: 0.58–0.71% of binder	-ICAR rheometer -Bingham model	-Dynamic yield stress: 250–500 Pa -Plastic viscosity: 22–60 Pa.s	Water/binder ratio and PP fiber content significantly affected rheology. Early-age shrinkage was rapid, reaching 96% within 24 h.
Souza et al. [116]	OPC, sucrose, commercial setting retarder (CSR), polycarboxylate ether-based superplasticizer (PCE), calcium chloride (CC), setting accelerator	-Water-to-cement ratio: 0.28–0.32, by cement weight: -CSR: 0–0.5%, -Sucrose: 0–0.5%, -PCE: 0–0.3%, -CC: 0–3.0%, -setting accelerator: 0–5.0%	-RheoWin HAAKE Viscotester iQ rheometer -Shear growth test for static yield stress	-Static yield stress: ~500–1800 Pa -Athix: 0.4–8.2 Pa/s	Setting retarders and superplasticizers improved open time but reduced buildability. Accelerators increased the structuration rate, but higher dosages were needed when used with superplasticizers.
Nerella et al. [117]	CEM I 52.5 R cement, FA, micro-silica suspension, SP, set accelerator	-Water-to-cement ratio: 0.42, -SP: 0–0.75% -Accelerator: 0–2.5% -Cement replacement with SCMs: 0–45% by volume	-HAAKE MARS II coaxial rheometer -Stress growth test -Bingham model	-Static yield stress: ~0–260 Pa (varying with composition and age) -Athix: 0.07–1.83 Pa/min	A strain-based approach for measuring structural build-up was proposed, prioritizing a constant effective strain $\geq$1.5 over a constant shear rate. This method better characterizes stiffer printable mixes.

Table 2. *Cont.*

Name	Materials	Material Parameters	Test Equipments/Models	Rheological Properties	Key Findings
Rubin et al. [118]	PC, natural quartz sand, limestone filler, SF, PCE, aluminum sulfate accelerator	-Water-to-cement: 0.35 -Water-to-binder: 0.32 -Accelerator dosage: 0–4% by cement weight -superplasticizer dosage: 0.003–0.007% by cement weight	-Direct shear test -Rotational rheometry (Schleibinger Viskomat XL)	-Static yield stress: ~2000–4000 Pa, -Athix: 0.67–9.66 Pa/s	Rotational rheometry yielded higher stress values than direct shear tests. Accelerators caused an exponential increase in yield stress at early ages. A new model for this exponential yield stress evolution was proposed, and an analytical model for predicting buildability was reviewed.
Chen et al. [119]	CSA, metakaolin, HPMC, WRA, tartaric acid, water.	-Water 0.35, -Metakaolin 0–3%	-Rotational rheometer (Kinexus lab+, Malvern) -Bingham and Herschel–Bulkley models	-Static yield stress: 150–675 Pa -Dynamic yield stress: 303–675 Pa -Plastic viscosity: 2.4–2.57 Pa.s	Metakaolin addition improved yielding behaviors and thixotropy of 3D-printed CSA cement composites, leading to decreased structure deformation. The Herschel–Bulkley model was more suitable for analyzing dynamic rheological properties than the Bingham model
Jayathilakage et al. [120]	Cement, graded coarse and fine sand, SF, SP, retarder, water	-Water/cement ratio: 0.25, -Variable: Layer width (20 mm and 30 mm nozzle sizes tested)	-Vane shear apparatus	-Initial yield stress: 300–1500 Pa	A Mohr–Coulomb-based buildability criterion was developed and validated, offering greater accuracy in predicting plastic collapse failure height.

3.2. Sustainable Binders

3.2.1. Geopolymer Inks

Geopolymers are predominantly fabricated using supplementary cementitious materials such as ground granulated blast furnace slag, fly ash, metakaolin, calcined clays, and zeolite, which are all rich in Al_2SiO_3 and Na_2SiO_3/NaOH (alkali-activated silica) solutions [121]. Instead of Portland cement, geopolymers reduce CO_2 emissions by using industrial by-products containing aluminosilicate phases with minimal environmental harm. Employing geopolymer in AM promotes sustainable development due to being an eco-friendly construction material [122,123]. Geopolymers, an alternative to Portland cement, reduce environmental damage and CO_2 emissions by integrating industrial by-products into their aluminosilicate structure. These materials, which reduce industrial waste and decrease environmental impact, exhibit low energy usage and CO_2 emissions. They are ideal for addressing the eco-friendly and sustainable requirements in contemporary building material production [124]. Panda et al. [122] investigated fly ash-based geopolymer cement for large-scale AM and found that the 3D-printed geopolymer maintains the inherent mechanical strengths of the material, making it highly suitable for sustainable construction. However, the anisotropic nature of 3D printing impacts the mechanical properties of geopolymers, depending on the direction of loading [122].

With its abundant aluminosilicate composition and superior performance compared to traditional cement concrete, geopolymer concrete shares traits similar to those of the cement family [125,126]. Geopolymer concrete has been reported to exhibit several advantageous characteristics, including rapid development of compressive strength [127,128]. Geopolymer concrete is composed of aluminosilicate materials that react with alkaline liquids to form a hardened binder, which contributes to its strength [125]. Furthermore, the addition of components like fly ash to geopolymer concrete mix not only makes use of industrial waste but also improves the concrete's durability and mechanical qualities [129].

Geopolymer concrete sets much faster, making it especially beneficial for 3D printing in concrete applications compared to OPC concrete. The geopolymerization process and materials used in geopolymer determine this trait. Under ambient conditions, high-strength geopolymer can rapidly set and attain adequate early strength [130,131]. This rapid setting time can be attributed to the high calcium oxide content in certain fly ash-based geopolymers, which may lead to flash setting or rapid hardening [132].

Geopolymer concrete has improved tensile strength, which is especially important for 3D-printed structures. The addition of polypropylene fibers improves its mechanical properties, with specimens containing 0.5% fiber showing the highest strength values [133,134]. Studies have also shown that geopolymer concrete is more resistant to acid attacks [135], chloride ion penetration, and freeze–thaw cycles, which are crucial for structures exposed to harsh environments [136,137]. After frost resistance tests, 3D-printed geopolymer materials demonstrated slightly lower strength but higher thermal conductivity compared to conventional concrete [138].

Geopolymer concrete has improved fire resistance [139], resistance to freeze–thaw cycling [140], insulating properties [141], minimal creep and drying shrinkage, as well as exceptional resistance to sodium sulfate [142], 10–30% lower material cost [143,144], and a lower global warming potential compared to OPC [145]. Different fibers, such as steel [146], glass [147], natural fibers [148], and polymeric [149] fibers, have been used to increase its strength.

Various institutions and firms have developed sustainable printable geopolymer concretes. For example, RENCA has produced and launched geopolymer 3D printing mortar for commercial use based on eco-friendly geopolymer technology [150]. Figure 3 shows different printable geopolymer matrices.

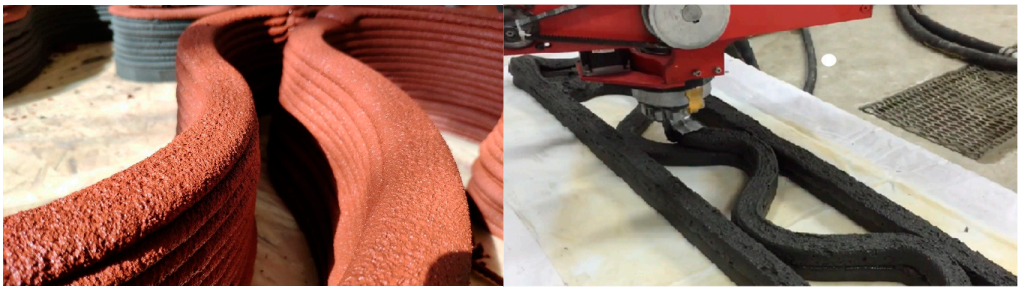


Figure 3. 3D printable geopolymer matrix [150].

Three-dimensional-printed geopolymer concretes, a more sustainable alternative to traditional Portland cement concretes for lowering CO_2 emissions, offer a reduced environmental impact [151,152]. Several research groups have investigated 3D printable geopolymer inks. The suitability of geopolymers for 3D concrete printing was investigated by Panda et al. [151]. A single-component geopolymer consisting of aluminosilicate precursor and solid alkaline solution was formulated, displaying a thixotropic property akin to traditional Portland cement. At Delft University of Technology [153], the optimal geopolymer mix design incorporating Class F fly ash and blast furnace slag for extrusion-based 3D printing was studied. Three-dimensional printing's most suitable binder composition is 80% fly ash and 20% slag. The larger the amount of slag, the shorter the geopolymer's setting time becomes, making it unsuitable for extrusion. Three-dimensional printers with fast performance require a shorter open time than the geopolymer's 33 min. The alkaline solution's ratio and composition significantly affected the geopolymer's initial setting time.

Mechanical properties of 3D-printed geopolymers can be significantly enhanced by incorporating continuous steel cables and short PVA fibers. Lim et al. [154]. reported a 290% increase in flexural strength by using micro steel cables during printing. These reinforcements improve compressive strength, ductility, and toughness [155,156].

Three-dimensional printable one-part geopolymer concrete's rheo-chemical properties were studied by Muthukrishnan et al. [157] via activator content, thixotropic additive (MAS), and retarder (sucrose) dosage investigations. The one-part geopolymer with a binder composition of 0.75 wt% MAS, 10 wt% activator, and 1.5 wt% sucrose had improved printing properties. Hojati et al. [158] have created a geopolymer using basalt sand and carbon fibers with potential for use as a 3D printing construction material on Mars. The NASA 3D Printed Habitat competition witnessed the creation of a beam, cylinder, and dome structure by the research group through successful 3D printing.

Panda et al. [159] explored the characteristics of alkali-activated slag (AAS) binders tailored for extrusion-based 3D printing. The AAS mixtures' fresh properties were enhanced by adding nanoclay (NC) and nucleation seeds. Incorporating 0.4% NC into the AAS mixtures augmented their thixotropic behavior, and adding 2% hydromagnesite seeds created more nucleation points, leading to a higher rate of hydrate phase precipitation. Consequently, the rate of structural build-up required for large-scale 3D printing saw improvement. This AAS formulation was successfully utilized to print a real 3D structure, affirming its practicality for 3D printing uses.

Future studies on 3D printing geopolymer concrete can investigate other polymers, such as polyacrylonitrile, polybutadiene, polystyrene, and polypropylene, alongside popular options like polylactic acid and polyethylene terephthalate glycol [160,161]. Additionally, the durability of polymers currently used in 3D printing for geopolymer matrices requires further exploration. Conducting a life cycle assessment (LCA) of geopolymer concrete will also be crucial in enhancing its sustainability [124]. In contrast to traditional cement-based materials, geopolymers present a more sustainable option due to their reliance on industrial by-products like fly ash and slag. These materials offer a lower environmental footprint, but understanding their behavior during the 3D printing process is crucial. Geopolymers exhibit unique rheological properties that influence their printability and structural stability. Table 3 provides an overview of various 3D-printed geopolymer formulations, outlining key factors such as composition and performance outcomes.

Table 3. Rheological properties of geopolymer-based 3D printable mixtures.

Name	Materials	Material Parameters	Test Equipments/Models	Rheological Properties	Key Findings
Panda et al. [162]	FA, GGBS, Potassium Silicate (K_2SiO_3), nanoclay (attapulgite clay), river sand,	-Activator-to-binder ratio: 0.35, -Water-to-solid ratio: 0.30, -Nanoclay content: 0.5%	-Stress growth test -Viscosity recovery test	-Static yield stress: ~1000 Pa -Viscosity recovery: ~1000 Pa	The study found that adding 0.5% nanoclay improved the yield stress and thixotropy of geopolymer mixes, enhancing their suitability for 3D printing applications.
Zhang et al. [163]	GGBS, steel slag, sodium metasilicate, Sodium Hydroxide (NAOH),	-Water/binder ratio: 0.35, -sodium metasilicate (20–40 g), -NAOH (0–20 g), -Si/Na ratio: 0.5–1.0	-Rheometer -Modified Bingham model	-Initial yield stress: 0.339–3.439 Pa, -Yield stress after 1–20 min rest: 1.71–5.30 Pa	The study found that lower Si/Na ratios led to higher yield stress and better structure-rebuilding ability, which are beneficial for 3D printing applications.
Zhou et al. [164]	FA, GGBS, residue soil (RS), river sand, Sodium Silicate (Na_2SiO_3), NAOH,	-Water/solid ratio: 0.42, -sand/solid ratio: 1.0, -water reducer: 10%, RS content: 0–110% of binder mass	-Rheometer, -Bingham model	-Static yield stress:1496.4–3196.6 Pa, -Dynamic yield stress: 131.9–504.6 Pa, -Plastic viscosity: 5.73–10.49 Pa.s	Increasing RS content led to higher yield stress and viscosity, improving shape retention and buildability for 3D printing, but excessive RS content (>90%) negatively affected extrudability and mechanical properties.
Paiva et al. [165]	Metakaolin, Potassium Hydroxide (KOH), K_2SiO_3, NaOH, Na_2SiO_3, natural sand	-Water/solids ratio: 0.40–0.50, -sand content: 0% or 40% volume per volume percent	-Rotational rheometer	-Static yield stress: ~400–4000 Pa (depending on composition and resting time)	Sodium-based activators produced geopolymers with higher initial yield stress compared to potassium-based activators. Lower water/solids ratios and sand addition improved rheological properties.

Table 3. *Cont.*

Name	Materials	Material Parameters	Test Equipments/Models	Rheological Properties	Key Findings
Panda et al. [166]	FA, GGBS, SF, Na_2SiO_3, NaOH, Solution/binder ratio: 0.46	-FA content: 90–100% -GGBS and SF contents: 0–10%	-MCR 102 rheometer	-Initial yield stress: ~330–660 Pa, -Thixotropy index (λ): 0.24–1.42 (after 1–20 min rest)	SF addition significantly improved yield stress and thixotropic behavior of geopolymer mixes, enhancing shape retention for 3D printing.
Sandoand Stephan [167]	FA, GGBS, Na_2SiO_3 solution, NaOH, fine aggregate (for mortar mixes),	-Activator/binder ratio: 0.20, -Water/binder ratio: 0.16	-Penetration test with Toni SET Force penetrometer	-Initial yield stress: ~2000–4000 Pa -Yield stress after 60 min: ~20,000–120,000 Pa	They highlight that mixing time significantly influences the printability of geopolymers. Shorter mixing durations lead to a stiffer consistency, which compromises extrudability and makes the material unsuitable for 3D printing applications.
Guo et al. [168]	FA, slag powder, SF, anhydrous Na_2SiO_3 powder, quartz sand, ATTAGEL-50	-10–30% slag powder -10–30% SF	-RVDV-2 type rotational viscometer -Bingham model, -Herschel–Bulkley model	-Apparent viscosity: ~10–70 Pa.s -Plastic viscosity: 5.5–8.80 Pa.s -Yield stress: 6.74–103.97 Pa	The addition of 10% slag powder and 10% SF improved the apparent viscosity and yield stress of the geopolymer mixture, enhancing its suitability for 3D printing. The Herschel–Bulkley model was found to be more accurate in characterizing the rheological behavior of the geopolymer mixtures compared to the Bingham model.

Table 3. *Cont.*

Name	Materials	Material Parameters	Test Equipments/Models	Rheological Properties	Key Findings
Zhu et al. [169]	FA, GGBS, sand, NaOH, Na_2SiO_3 solution, polyethylene (PE) fibers	-GGBS content: 100–300 g, -NaOH content: 27–58 g, -sand content: 400–800 g, -PE fiber volume: 0–0.6%	-Anton Paar MCR302 dynamic shear rheometer, -Herschel–Bulkley model	-Yield stress: 7.93–57.86 Pa	Increasing GGBS and sand content improved stacking performance and fluidity while increasing NaOH content improved stacking but reduced fluidity. Adding PE fibers significantly increased yield stress but slightly reduced flowability.
Brandvold and Kriven [170]	Metakaolin, K_2SiO_3 solution (potassium water glass)	-Temperature 5–55 °C -Shear rates: 25–100 s^{-1}	-Discovery Hybrid Rheometer 2	-Yield stress: 15.5–393.22 Pa -Viscosity: ~7–15 Pa.s	Temperature greatly affects rheology. Higher temperatures (35–55 °C) lower initial viscosity but cause rapid increases in viscosity and yield stress due to accelerated geopolymerization. Lower temperatures (5–15 °C) result in higher initial viscosity but more stable properties, providing longer printing windows.
Kashani and Ngo [171]	GGBS, FA, SF (ratios 3:1:0.5), sodium metasilicate powder,	-8 and 10% sodium metasilicate powder -0.31–0.35 w/s ratio	-Haake Rheometer (Viscotester 550)	-Initial yield stress: 680–1670 Pa	The optimal mixture (8 wt% activator, w/s ratio 0.33) exhibited suitable rheological properties for 3D printing with yield stress ~1400 Pa.

Table 3. *Cont.*

Name	Materials	Material Parameters	Test Equipments/Models	Rheological Properties	Key Findings
Shahmirzadi et al. [172]	FA, GGBS, lead smelter slag, Graphene Oxide (GO), Nanoclay	-GO: 0–0.07 wt%, -nanoclay:0–0.50 wt%, -FA ratio: 1.0:0.0–0.5:0.5, -activator/binder: 0.35–0.40, -activator modulus: 1.5–2.1 24–50%, -relative humidity (RH), 35–50%, 35–90%	-HAAKE Viscotester 550 rheometer, -Anton Paar MCR 702 TwinDrive rheometer	-Static yield stress: ~1000 -Apparent viscosity (from structural rebuilding test): ~5000–23,000 mPa.s	Incorporating GO at 0.03–0.07 wt% significantly improved yield stress development and viscosity recovery compared to nanoclay. GO-modified mixes showed superior rheological properties for 3D printing, with higher viscosity recovery (66.5% for 0.07% GO vs 55.8% for 0.5% nanoclay).
Lv et al. [173]	GGBS, sodium carboxymethyl starch (CMS) as a modifying agent, water glass, NaOH,	-Water/solid content: 0.37, -CMS content: 0–3% by weight of GGBS	-Anton Paar MCR-301 rheometer, -Bingham model, -Herschel–Bulkley model	-Yield stress: 0.99–23.87 Pa -Plastic viscosity: 0.05869–12.0394 Pa.s -Thixotropy: 88.70–3515.80 Pa/s	CMS significantly enhanced the rheological properties of alkali-activated slag paste, improving yield stress, plastic viscosity, and thixotropy, making it suitable for 3D extrusion forming.
Sariyev et al. [174]	FA, polypropylene (PP) fibers, Na_2SiO_3, NaOH (NaOH),	-Alkaline solution-to-binder ratio: 0.4, -PP fiber content: 0–1% by volume	-Anton Paar MCR 102 rotational rheometers, -Herschel–Bulkley	-Yield stress: 30–95 Pa, -Static yield stress range for optimal extrusion: 30–70 Pa	The optimal PP fiber content range of 0.25–0.5% provided balanced rheological properties for 3D printing, enhancing performance without complicating the extrusion process.

Table 3. *Cont.*

Name	Materials	Material Parameters	Test Equipments/Models	Rheological Properties	Key Findings
Chen et al. [175]	FA, GGBS, nanocellulose (Nano-fibrillated cellulose (NFC) and Micro-fibrillated cellulose (MFC)), magnesium oxide (MgO)	-MgO: 0–2%, -NFC: 0–2%, -MFC: 0–2%, -calm breeze and strong wind condition: ~0.03–0.05–0.1 kg/m^2/hr evaporation rate	-Viskomat XL concrete rheometer	-Yield stress: 37.12–79.68 Pa -Plastic viscosity: 1.84–2.64 Pa.s -Thixotropy: 1308–6158 Pa/s	Adding nanocellulose (NFC or MFC) significantly increased yield stress, plastic viscosity, and thixotropy of geopolymer paste, improving printability and buildability. NFC had a greater effect than MFC.
Saadati and Kani [176]	Phosphorous slag, Mullite (obtained from calcined kaolinite), Silica sand, NaOH, Na_2SiO_3,	-Sand/binder ratio: 0.6, -Liquid/solid ratio: 0.43, -Mullite content: 2–15% -Si/Na ratio: 0.2–0.6	-MCR 302 Anton Parr rheometer, -Herschel–Bulkley	-Yield stress: ~13–35 Pa -Plastic viscosity: 0.8–1.6 Pa -Apparent viscosity: ~2–30 Pa.s	Geopolymer pastes follow the Herschel–Bulkley fluid model and exhibit thixotropic behavior. The geopolymer mixture prepared with 5% mullite and a Si/Na ratio of 0.4 showed optimal rheological properties for 3D printing applications.
Brandvold et al. [177]	Metakaolin (Metamax HRM), K_2SiO_3 solution, sand, basalt fibers	-Sand content: 30–60 wt% -Basalt fiber length: 3.175–12.7 mm -Squeeze flow rate: 0.1–3.0 mm/s	-Discovery Hybrid Rheometer-2	-Yield stres: 2.77 Pa	Geopolymer composites with 50–60 wt% sand and 3 wt% basalt fiber exhibited rheological properties comparable to Ordinary Portland Cement (OPC), showing potential for 3D printing applications.

Table 3. *Cont.*

Name	Materials	Material Parameters	Test Equipments/Models	Rheological Properties	Key Findings
Brandvold et al. [178]	Metakaolin (MetaMax), K_2SiO_3 solution	-Shear rates: 10–250 s^{-1}, -Resting times: 0–140 min (in 10-min increments)	-Discovery Hybrid Rheometer-2	-Viscosity range: 1.95–5.79 Pa.s (at shear rates 10–50 s^{-1})	Geopolymer pastes exhibit strong thixotropic behavior, with full thixotropic restructuring occurring around 90–100 min of total undisturbed rest time. Reaching a state of full thixotropic disturbance heavily depends on subjected processing parameters.
Souza et al. [179]	Metakaolin, NaOH, Na_2SiO_3, additional water	-Na_2SiO_3: 6.4–33.9 wt%, -Additional water: 0–4.3 wt%	-HAAKE MARS III rheometer	-350–800 Pa Yield stress	Temperature manipulation can effectively control the reaction rate of geopolymers and their rheological properties during printing. High-fluid mixtures can be quickly turned into buildable ones through systematic heating.
Ma et al. [180]	Metakaolin-based geopolymers activated by Na+, K+, or Cs+ ions Triton X-100, PEG, PVA, and Kaolin as rheology modifiers	-Triton content: 0–2.50%, -PEG content: 0–3.75%, -PVA content: 0–3.75%, kaolin content: 0–60%	-DHR-1 rheometer (TA Instruments), -Bingham model, -Herschel–Bulkley model	-Yield stress range: 308.0–1765.9 Pa -Viscosity range: 28.3–180.7 Pa.s	The Triton–Kaolin rheology modifier combination demonstrated universality in rheological control of Na+-, K+-, and Cs+-based geopolymer inks, with the corresponding minimum slump rates of 0.7%, 0.4%, and 0.8%, respectively.

Table 3. *Cont.*

Name	Materials	Material Parameters	Test Equipments/Models	Rheological Properties	Key Findings
Ramakrishnan et al. [181]	Metakaolin, Na_2SiO_3, OPC, FA, GGBS, silica sand (fine and coarse), sucrose (1 wt% of binders as retarder)	-OPC (0–25% replacement of FA or slag)	-Viskomat XL rheometer	-Static yield stress range: 4.6–168.9 kPa (at 30 min)	Two-part printhead mixing of geopolymer and OPC slurries allows for rapid setting and strength development after extrusion while maintaining good pumpability. Replacing FA with 25% OPC showed the best performance, with 17× higher static yield stress.
Panda et al. [122]	FA, GGBS, SF, K_2SiO_3 solution, KOH, fine river sand, thixotropic additives (Actigel and cellulose).	-	-Viskomat XL rheometer, -Bingham model	-Thixotropic index: Minimum value of 10,000 (area between up and down curve of T-N graph)	The developed geopolymer mixture exhibited suitable rheological properties for 3D printing, with a printable thixotropic zone identified for extrusion-based applications.
Rahemipoor et al. [182]	FA, Microencapsulated Phase Change Materials (MEPCM), Na_2SiO_3, NaOH	-MEPCM content: 0–20 vol%	-Anton Paar Physica MCR 502 rheometer, -Bingham model	-Yield stress: ~30–530 Pa -Plastic viscosity: ~10–90 Pa.s	MEPCM served as both a thermal energy management component and a viscosity modifier for 3D printable geopolymer paste.

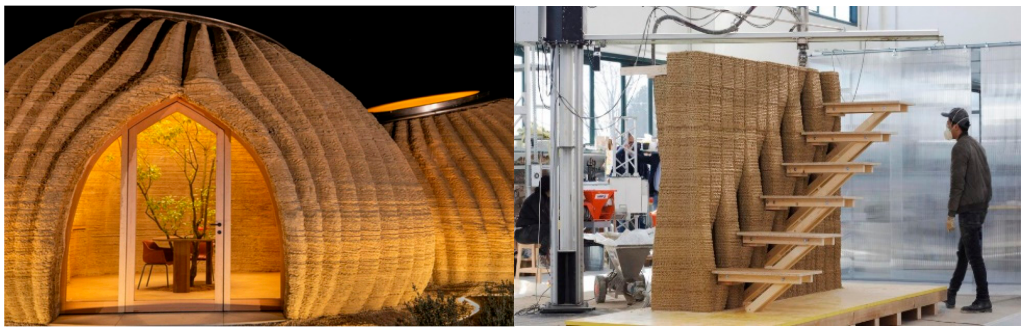
Table 3. *Cont.*

Name	Materials	Material Parameters	Test Equipments/Models	Rheological Properties	Key Findings
Ranjbar et al. [183]	FA, halloysite nanotube (HA), meta-halloysite (MHA) (calcined at 800 °C), Na_2SiO_3, NaOH, silica sand	-HA/MHA content: 0–15 wt% of FA	-Anton Paar Physica MCR 502 rheometer	-Static yield stress: ~1000–1700 Pa	Adding just 1–2 wt% halloysite significantly increased rheological properties and buildability of 3D printable geopolymer mortars without compromising mechanical strength. MHA accelerated setting time compared to untreated HA.
Sun et al. [184]	GGBS, Calcium carbonate powder, Na_2SiO_3, NaOH, CMS	-CMS content: 0–8% by weight of total solids, -Water-solid ratio: 28 wt%	-Anton Paar MCR 301 rotational rheometers, -Herschel–Bulkley model	-Plastic viscosity: 10.08–75 Pa.s, -Yield stress: ~1–70 Pa	The addition of CMS significantly enhanced the rheological properties of geopolymer composites, improving workability and shape retention during 3D printing. Optimal CMS content was found to be between 4% and 6%, which provided suitable viscosity and yield stress for extrusion.

3.2.2. Earth-Based Inks

For centuries, natural earth resources have been used to build structures worldwide. The integration of earth-based mixtures in new construction techniques appears advantageous due to several sustainable benefits, including resource efficiency [185]. These materials reduce energy consumption during production, possess thermal and humidity regulation properties, and improve energy efficiency and indoor air quality [186,187]. Using earth-based mixtures in innovative construction methods offers breathability [188], toxin absorption [189], recyclability, and zero waste [190]. Earth-based materials, known for regulating indoor climates and having a minimal environmental footprint, are gaining recognition [191,192].

Although 3D printing with earth-based materials is advancing, research on printability is limited. Three-dimensional-printed goblet-shaped TECLA shelter, crafted from recycled local terrain materials, boasts a novel circular design [193]. Additionally, Figure 4 shows wall prototypes and stairs at the Institute for Advanced Architecture of Catalonia (IAAC) used similar clay soil [194]. The printability of earth-based materials depends on pumpability, extrudability, and buildability. It is essential to balance printability improvements, such as adjusting fluidity and water content, with maintaining material strength [37].



(**a**) (**b**)

Figure 4. Types of earth-based 3D-printed paths [149] (**a**) goblet-shaped TECLA shelter (**b**) wall prototypes and stairs with clay soil at IAAC.

While most research in 3D printing construction focuses on cement-based materials, Bajpayee et al. [195] introduced a new palette of natural soils for AM, including a burlewash clay crosslinked into a siloxane framework. To ensure the development of a new palette for sustainable construction materials, the importance of an integrated LCA approach is emphasised. Curth et al. [196] suggest recommendations for sourcing, treating, and characterizing local earthen materials based on factors like soil type, moisture content, fiber content, and compressive strength. Full-scale wall prototypes were created using a six-axis robotic printing machine, and an LCA showed that earth-based AM is environmentally competitive with other methods.

In a review of 3D printing with soil-based materials (2000–2019), Arrieta–Escobar et al. [197] identified key challenges and prospects, such as biocompatibility, chemical and mechanical stability, and spatial resolution. Perrot et al. [198] improved the green strength and printability of earthen structures by incorporating alginate seaweed biopolymers into raw earth, achieving compressive strength comparable to cob earth. Gomaa et al. [199] reviewed the potential of earth-based materials like clay, soil, and adobe in 3D printing for sustainable construction, highlighting their properties and environmental benefits. To further explore the potential of 3D-printed earth-based mixtures, understanding their rheology is critical. Table 4 details the rheological properties of various formulations, providing insights for optimizing printability and structural integrity.

Table 4. Rheological properties of earth-based 3D printable mixtures.

Name	Materials	Material Parameters	Test Standards/Equipments/Models	Rheological Properties	Key Findings
Biggerstaff et al. [200]	Lunar regolith simulant (JSC-1A), bovine blood proteins (AP920), deionized water	-Biopolymer solution concentration: 34.5–37.9%, -biopolymer–soil ratio: 10–19.9%, -moisture content: 15.5–36.7%	-ASTM C230, ASTM C1437 minicone slump test, -cylindrical slump test, -elastic–plastic slump model	-Dynamic yield stress: 8–1438 Pa -Static yield stress: 52–1438 Pa	The post-printing height of a 3D-printed biopolymer-bound soil composite layer can be accurately predicted using an elastic–plastic slump model based on yield stress, wet elastic modulus, and density.
Alqenaee and Memari [201]	Clay, sand, water, lime, straw	-Clay: 38.5–52.6%, -Sand: 11.1–17.7%, -Water: 24.2–34.3%, -Lime: 7.4–11.6%, -Straw: 0–1.5%	ASTM D4318–17 Plasticity test: hand rolling procedure for workability	Printability and buildability were evaluated qualitatively through printing tests	The optimal printable mixture contained 49% clay, 24.2% water, 15.3% sand, 10% lime, and 1.5% straw. Three-dimensional-printed specimens generally showed higher strength than cast specimens.
Ji et al. [202]	Four different soils, flax fiber, sand	-Clay: 4–31%, -Silt: 11–41%, -Sand: 39–80%, -Water content: 18–45%	-Fall cone test	-Yield stress: max 2000 Pa (varies with water content)	Shrinkage is reduced by decreasing water content and increasing sand content. Extrudable mixtures had yield stress < 2000 Pa for Guerande soil and <1500 Pa for Ballan Mire soil.
Perrot et al. [198]	Raw earth, alginate (Cimalgin HS_3)	-Earth: 100%, -Water: 45%, -Alginate: 3% (of earth mass)	-Vane test for yield stress measurement, -penetration test for green strength and elastic modulus.	Initial yield stress: 1500 Pa	The addition of alginate allowed for the rapid development of green strength, enabling the printing of a 3 m-high wall in 1 day.

Table 4. *Cont.*

Name	Materials	Material Parameters	Test Standards/Equipments/Models	Rheological Properties	Key Findings
Asaf et al. [203]	Sand, kaolinite clay (white, chocolate, and Mamshit varieties)	-Clay content: 19.4–33%, -Sand content: 49.1–65.5%, -Water content: 15.1–18.2%	-ICAR Plus rotational rheometer	-Static yield stress: ~1000–3000 Pa, -Dynamic yield stress: ~500–2000 Pa -Apparent viscosity: ~5–20 Pa.s	Flow table spread and rigidity coefficient correlate strongly with pumpability and stability. Higher kaolinite content enhances thixotropy, while coarser particles increase static yield. An analytical model based on rheological properties accurately predicted cylinder collapse during printing. Optimal mixtures balanced flowability and stability, with 28.6% clay content performing best.
Benzerara et al. [204]	Raw earth, diss fibers, date palm tree fibers, xanthan gum (XG), sodium hexametaphosphate (HMP)	-Earth: 49.1–65.5%, -Fibers: 1.5–3% by volume, -Water: 23–28%, -XG: 0.5–2% of dry earth mass, -HMP: 0.3% of dry earth mass	-ASTM D4318 Cone penetrometry test	-	It was found that the materials tested could be extruded when the depth of penetration varied between 3 and 5 mm.
Biggerstaff et al. [205]	JSC-1A lunar regolith simulant, bovine blood proteins (AP920), deionized water	-Biopolymer solution concentration: 34.5–37.9%, -Biopolymer–soil ratio: 10–19.9%, -Moisture content: 15.5–36.7%, -Soil volume fraction: 0.321–0.548	-Steady stress sweep test, -constant shear rate test with ARES-G2 Rheometer	-Static yield stress: 46–3644 Pa, -Dynamic yield stress: 6–3786 Pa	Soil volume fraction range of 0.435–0.548 was identified as suitable for 3D printing based on extrudability and shape stability requirements. The Chateau–Ovarlez–Trung model accurately predicted dynamic yield stress up to a soil volume fraction of 0.52, while De Larrard's model better predicted static yield stress across the full range.

Table 4. *Cont.*

Name	Materials	Material Parameters	Test Standarts/Equipments/Models	Rheological Properties	Key Findings
Maierdan et al. [206]	Kaolinite clay, sodium alginate, distilled water	-Kaolinite content: 40–120 g per 50 g water, -Alginate content: 0–2.4% by mass of water	-TA DHR 20 Rheometer with vane geometry	-Static yield stress: ~10–450 Pa, -Dynamic yield stress: ~10–300 Pa	Sodium alginate increased electrostatic repulsion between kaolinite particles, reducing flocculation and sedimentation. This decreased yield stress and storage modulus by orders of magnitude at low alginate contents. Above a critical concentration of 0.12–0.6%, alginate formed a polymer network that increased yield stress and modulus. Alginate addition shifted the printable clay content range to higher values, with potential benefits for strength and shrinkage.
Maierdan et al. [207]	Kaolinite clay, XG, water, sand (for compressive strength tests only)	-Water/clay ratio: 0.83–1.25, -XG concentration: 0–5.5% by weight of water	-TA DHR 20 rheometer with vane geometry, -Bingham model	Not specified for "Printable" mixture (5% XG, 0.83 water/clay ratio)	XG initially disperses clay particles, decreasing yield stress and viscosity. Above 0.6% concentration, XG forms a polymer network, increasing these properties and enabling 3D printability at 5% XG content.

Table 4. *Cont.*

Name	Materials	Material Parameters	Test Standards/Equipments/Models	Rheological Properties	Key Findings
Tarhan et al. [208]	Raw earth (RE), quarry wash mud (QWM), sea sand (SS),	-RE: 44%, -QWM: 16%, -SS: 40%, -Water: 21%	-Fall cone test (EN ISO 17892-6), -Vane shear test (ASTM D4648/D4648M-16, RheolabQC SN80518563 rotational rheometer	-Yield stress: 806.31 Pa (fall cone test), -Shear strength: 1590 Pa (vane shear test)	The earth-based mixture demonstrated remarkable stability with consistent shear strength values, ensuring its rheological properties remained unchanged, allowing for long-term, uninterrupted construction without concerns about flow variations. A lime-based mixture was also developed, becoming workable after a second mixing, highlighting the importance of proper mixing for rheological purposes.

Housing has a big impact on the Indian economy, but there is a shortage of 27 million units, mostly affecting the middle class and economically disadvantaged groups. Without action, this deficit is expected to reach 38 million units by 2030. Using local expertise and technology to reduce construction costs without sacrificing quality is a potential solution for affordable housing. Raj et al. [209] also examined the use of 3D concrete printers and prefabricated concrete methods in low-cost housing. Because of problems with time, effort, and durability, fire bricks are frequently used in hot, arid countries like Egypt in place of earthen materials. El-Mahdy et al. [210] presented SaltBlock, a sand- and salt-based sustainable building technique. The process uses 3D printing to create an affordable composite while revitalizing the classic Karshif substance. For a 20 cm wall, SaltBlock prototypes outperformed fire bricks in terms of thermal performance (0.94 W/m²K) and compressive strength (9.5 MPa). In desert regions, this research encourages sustainable construction.

Biopolymer-bound soil composites (BSC) are a unique class of construction materials with potential use in sustainable construction on Earth and the creation of infrastructure on other planets. Biggerstaff et al. [205] conducted research on BSC and found that combinations, including proteins as biopolymers and polysaccharides, increase the soil's cohesiveness level. They also emphasized the need for a deeper understanding of the rheological characteristics and applicability of extrusion-based 3D printing within a soil volume fraction range of $0.435 \leq \phi BSC \leq 0.548$. Biggerstaff et al. [205] demonstrated that a BSC with low-cohesion soil is suitable for extrusion-based 3D printing.

The creation of an environmentally acceptable earth composite reinforced with natural sisal fibers and chemically stabilized using a hydraulic binder was studied by Silva et al. [211]. In order to determine the ideal water content, they also used shear vane experiments on new earth samples to analyze workability. Layer-by-layer deposition was made possible by the acceleration of the hardening process by the use of OPC as a chemical stabiliser. According to Silva et al.'s [211] findings, the shear yield strength is significantly influenced by the water content, fiber addition, and OPC replacement. This inexpensive, environmentally friendly earth-based composite can be utilized for 3D printing.

Integrating 3D printing with local resources for building construction is advancing rapidly. However, challenges such as material compatibility, process optimization, and verification of structural integrity continue to hinder widespread adoption. Nevertheless, the anticipated expansion of this technology promises to transform construction practices on Earth and, possibly, in extraterrestrial environments.

3.3. Sustainable Cementitious (Including SCMs) Binders

The phrase "cement-based composites" refers to a wider variety of materials than just "cement". Many studies have integrated mineral additives to create sustainable, cement-based, 3D printable concrete mixes that improve their engineering properties [42,44,49,54,212,213]. Incorporating mineral supplements into cement-based concrete for 3D printing boosts both its sustainability and engineering properties. Studies have explored various mineral additives like metakaolin, micro-silica, slag, fly ash, and rice husk ash. Three-dimensional concrete printing is enhanced through the addition of certain substances, resulting in improved pumpability, printability, buildability, and mechanical performance, as well as a reduced environmental impact from high Portland cement content [49,63,214].

Chen et al. [215] reported a maximum of 45% substitution of cement with a mix of fly ash and silica fume for producing sustainable 3D printable concrete, while calcined clay is another viable option as a substitute. Le et al. [42] developed a 3D-printed mortar reinforced with polypropylene fibers, made of Portland cement, fly ash, silica fume, and

sand, containing superplasticizers and retarders for a 9 mm nozzle, workability of 100 min, and the ability to create 61 layers, resulting in a height of approximately 400 mm.

Advancements in low-clinker cement formulations greatly reduce the construction industry's environmental impact. The integration of SCMs into concrete reduces carbon emissions while improving its mechanical properties and durability [216,217]. Incorporating SCMs in concrete not just reduces carbon emissions but also improves the concrete's mechanical properties and durability. Boscaro et al. [216] produced cement with 50% Portland cement and 50% limestone, burnt oil shale, and fly ash as SCMs. This low-clinker mortar can be efficiently retarded, processed, pumped, and extruded immediately after mixing with the accelerator paste. Also, 303 kg/m^3 of Portland cement is needed for this mortar mix, which is almost half the usual quantity in digital concrete fabrication. Functionally graded concrete reduces the self-weight and consumption of materials in specific locations within concrete structures.

Craveiro et al. [218] created five functional concrete mixtures using a superplasticizer, chemical powder, and varying proportions of cork granules as aggregate substitutes, producing 3D printable, functionally graded construction elements. Chen et al. [219] applied a viscosity-modifying admixture to improve the printability of limestone-calcined clay-based cementitious materials. The researchers explored how an HPMC-based VMA affected the 3D printability and mechanical properties of the materials. Three-dimensional printability and mechanical performance were significantly enhanced when 0.24% VMA was added to the binder mass.

Using the LSD AM technique, water-resistant green bodies with high compressive strength have been produced. A 30.8 $\pm$ 2.5 MPa compressive strength has been achieved in green bodies by incorporating a polymeric binder during the LSD process. This figure matches or exceeds that of conventional concrete [220]. Noteworthy is the development's ability to highlight LSD AM techniques' capacity to create durable ceramic components for various applications, including autonomous Mars habitat fabrication. Moreover, Hojati et al. [158] used the MgO and $MgCl_2$ salts present in Martian soil to create Sorel cement, also referred to as Magnesium Oxychloride cement for Mars applications. By combining the binder with a magnesium chloride solution, they created a substance that looks like rock, sets quickly, and has a significant initial strength.

Limestone powder positively impacts the rheology, strength, and shrinkage properties of alkali-activated slag/fly ash grouting materials [221], in addition to the workability and pore structure of cement mortar [222]. But using too much may result in lower compressive strength in mortar [222]. The addition of limestone powder accelerates structural build-up in alkali-activated systems. Dai et al. [223] investigated the influence of limestone powder on alkali-activated cement in terms of rheological properties, pore chemistry, mechanical strengths, and microstructures. The addition of more limestone powder increased the rate of structural development in the ternary alkali-activated system. The thick water film and spherical shape of fly ash particles lead to increased particle packing and subsequently lower plastic viscosity. Introducing limestone powder weakened the compressive strength. Additionally, limestone powder has been recognized for enhancing the rheology, strength, and shrinkage properties of alkali-activated slag/fly ash grouting materials [221] and for improving the workability and pore structure of cement mortar [222]. Nonetheless, a higher limestone powder content has been linked to lower compressive strength in mortar [222].

The addition of magnesium oxide (MgO) to slag-based mixtures for environmentally friendly spray-based 3D printing has an impact on the concrete's hydration, rheological characteristics, and setting time. MgO considerably reduces the first setting time of fresh mixtures, according to Lu et al. [25], who observed a 78% reduction when 40% of ground granulated blast-furnace slag (GGBS) is replaced with MgO. Moreover, the rheological

characteristics are changed by the addition of fly ash cenosphere (FAC), which raises critical ratios and lowers pumping pressures to improve the quality of spray printing. On the other hand, according to Chen et al. [224], adding MgO to cementitious materials based on alkali-activated slag improves volumetric stability and reduces the heat of hydration; the most effective MgO content is less than 1%.

3.4. Foam Concrete

Three-dimensional printing research in the construction industry now includes foams as a crucial component [225]. Foam concrete is a versatile material that serves both structural and insulation functions [226]. Recently, foams have gained significance in the construction industry and have been incorporated into 3D printing research. Foam concrete, in comparison to lightweight concrete, is considered a versatile material suitable for both structural and insulation purposes. Their versatility in adapting to specific applications makes them even more desirable as materials.

There are many different techniques for introducing gas into a material. To date, direct blowing techniques are the most appropriate for extrusion printing and spray printing. Typical blowing agents include nitrogen, carbon dioxide, water, air, pentane, hexane, dichloroethane, and freon [227]. Some possible foams for 3D printing are polyurethane (PU), extruded polystyrene (XPS), expanded polystyrene (EPS), foamed glass, cement foam, and silica foam [225].

The foam concrete density ranges from 200 kg/m^3 to 2000 kg/m^3. It contains cement, water, preformed foam, fine sand, and mineral additives such as fly ash, silica fume, and other necessary chemical additives. Lightness and low density [228], thermal insulating properties [229], good resistance against fire [230], improved workability [231], cost-effectiveness [232], higher sound-absorbing rate, and poor mechanical strength are peculiar characteristics of foamed concrete [233]. It is most suitable for facade applications. Compared to similar highly insulating mineral materials such as aerated concrete, foam concrete is strain hardening, so the production process is eco-friendly thanks to its low energy consumption [234]. Foam bubbles are described as enclosed air voids formed by foam agents. Foam agents are synthetic, protein-based detergents, glue resins, hydrolysed proteins, resin soap, and saponin. Water-reducing admixtures are not typically used because they are likely to cause foam instability. In practice, foam concrete has been widely used in construction and building applications in various countries such as Germany, the UK, the Philippines, Türkiye, and Thailand [235].

The use of foam concrete in AM applications has been infrequently explored in the literature [35,225,226,233,234,236–238]. Lublasser et al. [234] examined the application of foam concrete on the bare walls of existing buildings to achieve a facade finish that is highly insulating, easily recyclable, and customizable due to the raw material mixture's properties. This study aims to ensure controllable and reproducible applications by focusing on the automated application of foam concrete using a robotic setup.

Further, 3DP-LWFC and classical foamed concrete were compared in their fresh state properties and mechanical strength by Falliano et al. [236]. The former's mechanical strength values significantly improved, with compressive strength increasing by over 70% and flexural strength by approximately 100%, when mixing intensity increased from 1200 rpm to 3000 rpm. Markin et al. [226] studied different printable foam concretes with densities ranging from 800 kg/m^3 to 1200 kg/m^3. The study examined the fresh and hardened state properties of foam concrete and evaluated its application in 3D printing in terms of its economic, sociological, and ecological impacts. Liu et al. [238] improved the printability of fresh foamed concrete (FC) using SAC. Moreover, 3DPFC's fresh properties, such as foam stability, open time, buildability, interlayer interface, porosity, and mechanical

anisotropy, were studied in relation to varying SAC compositions. Adding SAC expedites pore structure formation by enhancing hydration, thereby reducing FC settlement and hindering defoaming.

4. Research Findings

4.1. Yield Stress and Structural Stability

In 3D printable mixtures, yield stress is crucial for determining the structural stability of printed layers. High yield stress ensures that the material retains its shape during printing and resists deformation under its own weight. However, excessively high yield stress can hinder extrusion. As highlighted in Table 2, cementitious binders typically display a broad range of yield stress values (15 Pa to 6500 Pa), depending on the binder type and the use of supplementary materials such as FA, nanoclay, or SF. The addition of SAC, PP fibers, FA, ground granulated blast furnace slag (GGBS), SF, or nanoclay further enhances green strength, making these mixtures more suitable for 3D printing applications where structural integrity is essential.

Studies (Table 3) show that geopolymers generally exhibit lower yield stress values compared to cement-based mixtures but still provide adequate structural stability for 3D printing. Zhang et al. [163] and Paiva et al. [165] reported that lower Si/Na ratios and sodium-based activators lead to higher yield stress and improved structure recovery compared to potassium-based activators, making these mixtures more suitable for 3D printing. The incorporation of nanoclay or PP fibers further enhances the yield stress and buildability of geopolymer mixtures, improving their suitability for vertical constructions.

Earth-based mixtures show considerable variation in yield stress, influenced by the raw earth type, moisture content, and fiber reinforcements, with generally lower yield stress values compared to cementitious and geopolymer-based mixtures. However, the addition of biopolymers or fibers, as seen in studies by Biggerstaff et al. [205] and Perrot et al. [198], significantly improves structural stability by increasing yield stress and promoting rapid green strength development, which is critical for large-scale printing. Sodium alginate, at low concentrations, reduces yield stress by preventing flocculation and sedimentation through enhanced electrostatic repulsion between kaolinite particles. At higher concentrations (0.12–0.6%), it forms a polymer network that increases yield stress. Similarly, XG initially disperses clay particles, reducing yield stress and viscosity, but at concentrations above 0.6%, it forms a polymer network that enhances these properties, enabling 3D printability at 5% XG content.

4.2. Viscosity and Flow Behavior

Optimizing viscosity for 3D-printed mixtures requires balancing flowability and buildability across different material types. While high viscosity improves shape retention and ensures layers maintain their form after extrusion, excessive viscosity can hinder extrusion and pumping, complicating printability. Therefore, careful selection of water reducers, activators, or other additives is crucial to achieve the right consistency for smooth extrusion while still ensuring structural integrity throughout the printing process.

The viscosity of cementitious mixtures is critical for determining their flow behavior during 3D printing. In cement-based mixtures, viscosity typically ranges between 1.5 Pa·s and 62.1 Pa·s, depending on the material composition. As noted in studies by Zhang et al. [52] and Rubio et al. [97], mixtures with higher SF content generally show increased viscosity. This is due to the fine particles in SF, which reduce the water content and create a denser, less flowable mixture. However, careful control of the water-to-cement ratio and the use of SP can mitigate this effect, ensuring the mixture remains extrudable while retaining its shape post-extrusion. Limestone can lower the viscosity of CSA mixtures,

and the addition of 2% bentonite optimizes 3D printability by keeping plastic viscosity below 2.50 Pa·s and dynamic yield stress under 645.54 Pa. Bentonite enhances structural stability and minimizes deformation over time, making the material highly suitable for 3D printing.

Geopolymer mixtures, typically based on FA and GGBS, exhibit distinct viscosity characteristics due to the influence of alkali activators and supplementary materials like nanoclay and metakaolin. According to Panda et al. [162], Guo et al. [164], and Kashani and Ngo [167], adding SF and reducing the activator-to-binder ratio increases viscosity, which helps with shape retention during printing but decreases flowability. Geopolymer mixtures are also sensitive to the type of activator used, with sodium-based activators generally resulting in higher viscosity and yield stress compared to potassium-based activators, as noted by Paiva et al. [124]. Zhu et al. [165] found that higher GGBS and sand content improve both stacking ability and fluidity, while increasing NaOH content improves stacking but reduces flow. The addition of PE fibers increases yield stress but slightly limits flowability. Souza et al. [175] emphasized that adjusting the temperature can quickly enhance the buildability of fluid geopolymer mixtures during printing, as heating accelerates the transition from a highly fluid state to a buildable one. Brandvold and Kriven [166] also observed that higher temperatures (35–55 °C) initially lower viscosity but quickly increase yield stress due to rapid geopolymerization. In contrast, lower temperatures (5–15 °C) provide higher initial viscosity and more stable properties, allowing for a longer working time during printing. In earth-based 3D printable mixtures, viscosity and flow behavior are influenced by the natural variability of soils and the inclusion of fibers or biopolymers. As shown in the study by Asaf et al. [203], increasing the water content reduces viscosity, improving flowability.

4.3. Thixotropy and Material Recovery

Thixotropy, the ability of a material to recover its internal structure after shear stress, is crucial in 3D printing. It ensures strong interlayer bonding, shape retention, and structural stability during the printing process. However, achieving the right balance between thixotropy and flowability is essential to maintain both extrudability and buildability. This balance applies to all 3D printing materials, including cement-based, geopolymer, and earth-based mixtures, each of which presents unique challenges depending on their composition and the additives used.

In cement-based mixtures, high thixotropy ensures that the material can recover its internal structure quickly after deposition, which is vital for achieving strong interlayer bonding and shape retention. However, excessive thixotropy can hinder flowability, making pumpability a critical factor to optimize during formulation. A balance must be managed between buildability and extrudability. The inclusion of nanoclay, as seen in studies like [54,101,108–110], improves the thixotropy. Furthermore, Qian and De Schutter [109] report that the combination of nanoclay and PCE enables low dynamic yield stress while maintaining high thixotropy, making it ideal for 3D printing applications. This balance allows the material to flow easily during extrusion and quickly regain its structure afterward, ensuring strong layer adhesion and stability. Chen et al. [119] reveal that the addition of metakaolin improves yield behavior and thixotropy in 3D-printed CSA cement composites, reducing structural deformation and enhancing material stability during printing. Mohan et al. [97] borax extends open time in CSA mixtures, while limestone lowers viscosity and pumping pressure, improving buildability compared to Portland cement. Tarhan and Sahin [20] explore that the air-entraining admixture reduces yield stress and viscosity, improving flowability and extrusion. This finding is interesting in that it also

increases thixotropy, allowing a strong but previously hard-to-print mortar to become more extrudable without sacrificing structural stability, making it ideal for 3D printing.

Measuring and understanding the thixotropic behavior of geopolymer mixtures is also critical due to their unique chemistry and reliance on alkali activators. SF and nanoclay enhance thixotropic behavior [162,166,168,171]. Furthermore, graphene oxide (GO) at 0.03–0.07 wt% enhances yield stress and viscosity recovery better than nanoclay [172]. The use of thixotropic additives like sodium carboxymethyl starch (CMS) further improves these properties, though it may slow down the geopolymerization process due to water retention [173,184]. Nanocellulose (NFC or MFC) boosts yield stress, viscosity, and thixotropy in geopolymer paste, with NFC showing a stronger effect than MFC [175]. The study by Ranjbar et al. [183] reveals that adding 1–2 wt% halloysite improved rheology and buildability of geopolymer mortars while maintaining strength, with MHA accelerating the setting time compared to untreated HA. These additives enhance the geopolymer's ability to recover after shear stress, ensuring the printed layers maintain their shape while curing. On the other hand, thixotropic behavior also heavily depends on processing parameters such as resting time [178].

The thixotropic behavior of earth-based mixtures is primarily driven by the type and concentration of additives, such as biopolymers and kaolinite clay. In early work, Perrot et al. [198] demonstrated that alginate significantly increased the green strength of mixtures, enabling rapid large-scale construction, such as a 3 m-high wall built in a single day. This research underscored the material's potential for efficient 3D printing applications. Asaf et al. [203] later revealed that higher kaolinite content improves post-deposition structural integrity, which is crucial for maintaining layer stability during printing. Their findings suggested that optimizing clay content could effectively balance flowability and rigidity for better construction outcomes. Maierdan et al. [206] expanded on this by focusing on the role of sodium alginate as a biopolymer stabilizer. They found that alginate enhanced electrostatic interactions in kaolinite suspensions, reducing yield stress and enabling smoother extrusion. This also shifted the printability window to higher solid contents, leading to stronger printed layers and less shrinkage. In addition, natural fibers such as flax provide additional tensile strength and improve the thixotropy of the mixture, allowing for smoother material recovery after extrusion and decreasing shrinkage, per Ji et al. [202]. However, excessive fiber or biopolymer content can increase viscosity, making the mixture more difficult to extrude. Collectively, these studies highlight the importance of managing the clay–water ratio and additive concentrations to optimize the printability and mechanical performance of earth-based mixtures.

By analyzing the thixotropic behavior across cementitious, geopolymer, and earth-based mixtures, it is clear that thixotropy plays a central role in determining the printability, buildability, and structural stability of 3D-printed materials. Each material type offers unique advantages and challenges, with additives and supplementary materials significantly influencing their performance in 3D printing applications.

5. Future Work

5.1. Advancing Sustainability in Materials and Design

To further enhance the environmental sustainability of 3D printing in construction, future research should prioritize optimizing structural design models using sustainable materials. A crucial focus must be placed on determining the optimum mixture types for 3D printing that balance ecological impacts with performance. Currently, printable mixtures rely heavily on fine aggregates, often leading to increased CO_2 emissions and energy consumption due to their high binder content. This requirement leads to higher CO_2 emissions and increased energy consumption compared to conventional concrete due to the

higher binder content. Research should aim to improve the sustainability advantages of 3D printable concrete by exploring alternative materials beyond traditional cement. A missing direction is the use of geopolymers, SCMs, foamed concretes, and earth-based materials, which offer lower environmental footprints. Studies, such as Bhattacherjee et al. [32], have shown that ternary binders with high dosages of SCMs and geopolymers could significantly reduce CO_2 emissions and energy consumption compared to conventional concrete. Future work should extend the LCA of these materials to better understand their long-term sustainability.

Investigating the use of natural fibers as sustainable replacements for synthetic fibers in cementitious and cement-free 3D-printed concrete is another priority. Natural fibers enhance mechanical properties and reduce material weight, but their alkaline sensitivity poses challenges to long-term durability. Future studies should evaluate the impact of natural fibers on rheology, printability, and structural integrity, as well as their role in improving corrosion resistance and long-term performance [239]. Moreover, natural fibers have demonstrated a positive influence on the rheological properties of cement-based systems, improving printability and reducing water drainage during extrusion [240].

5.2. Enhancing Durability, Reinforcement, and Technological Frontiers

The microstructure and durability of 3D-printed concrete differ from traditional concrete due to increased porosity and cracking. Research should focus on understanding degradation mechanisms and their effects on the mechanical and micro-structural performance of cement-free printed samples. Furthermore, reinforcement strategies need to be integrated into automation systems to meet the structural demands of 3D-printed buildings. These strategies should address reinforcement requirements for shear, flexural, and torsional stresses [38,208], ensuring that 3D-printed structures achieve the desired ductility. Although diverse reinforcement methods exist, such as the use of alkali-resistant glass textiles and Shotcrete 3D Printing, more work is needed to ensure comparable flexural behavior to cast specimens [241,242].

The evolution of 3D printing toward 4D printing offers new possibilities, including adaptable structures with time-based functionality [8]. There is also research for shelters on the surface of the moon, which were printed in 3D with “lunar concrete”. The main ingredient in the mixture is powdery soil found all over the surface of the moon, known as the lunar regolith. Scientists from the Technical University of Braunschweig and Laser Zentrum Hannover (LZH) developed 3D-printed lunar regolith under zero gravity for the first time. The team’s MOONRISE laser can be mounted onto a lunar rover to fabricate long-term structures on the moon [243].

6. Conclusions

The integration of 3D printing technology in the construction industry represents a transformative shift towards more sustainable, efficient, and innovative building practices. This study reviewed various binder matrices, including cementitious and sustainable alternatives such as geopolymers and earth-based inks, highlighting their unique properties, environmental impacts, benefits, and challenges. Cementitious mixtures remain dominant in terms of research interest, as revealed by the substantial number of publications, due to their established mechanical strength and durability. However, their high carbon footprint underscores the pressing need for alternative materials to align construction practices with global sustainability goals.

In 3D-printed materials, yield stress, viscosity, and thixotropy are critical factors that influence printability and structural stability. Cementitious mixtures, despite their inherently high yield stress, can achieve suitable extrusion characteristics with the inclusion

of additives such as nanoclay and fibers, which enhance green strength and printability. Cementitious binders, predominantly based on Portland cement, continue to play a vital role in 3D printing construction due to their superior mechanical strength and durability. However, their significant environmental impact—primarily the high CO_2 emissions from cement production—underscores the urgent need to explore alternative materials. Innovative formulations, including CSA and alkali-activated materials such as fly ash and slag, have demonstrated the potential for significantly reducing the carbon footprint while maintaining the mechanical properties required for structural applications.

Geopolymers, with lower yield stress, offer an eco-friendly alternative. Geopolymers, utilizing industrial by-products like fly ash and slag, emerged as a promising alternative with lower environmental impacts. However, their adoption requires further research to address challenges such as anisotropic behavior and the optimization of mix designs for large-scale applications. These findings suggest that geopolymers could play a central role in reducing the environmental footprint of construction.

Earth-based mixtures also benefit from biopolymers and natural fibers, improving rheological properties and enabling the use of local materials, which lowers transportation-related emissions. However, managing yield stress is essential to balance printability and buildability, particularly due to the variability in the moisture content of local resources.

Foam concrete, with its dual-purpose structural and insulating capabilities, was also identified as a versatile material. Future research should focus on optimizing its formulation for consistent print quality, paving the way for energy-efficient and cost-effective construction solutions.

To enhance the sustainability and efficiency of 3D printing in construction, future research should focus on several key areas:

- Material innovation: Developing new binder materials with lower environmental impact, improved mechanical properties, and enhanced printability is crucial. This includes exploring the use of natural fibers, optimizing the mix design of sustainable binders, and investigating new polymers for reinforcement.
- Lifecycle assessment: Conducting comprehensive lifecycle assessments of 3D-printed structures will provide valuable insights into their long-term sustainability and environmental impact. This will help identify areas for improvement and promote the adoption of green materials and processes.
- Design and simulation tools: Enhancing computer-aided design (CAD) systems and simulation tools tailored for additive manufacturing will streamline the design process and improve the accuracy and efficiency of 3D printing in construction.
- Automation and reinforcement: Integrating reinforcement strategies into automated printing systems will address the structural demands of 3D-printed buildings. Research should focus on optimizing the placement and type of reinforcements to ensure the structural integrity of printed structures.

Three-dimensional printing technology holds great promise for the construction industry, offering opportunities for sustainability, efficiency, and innovation. By continuing to innovate in material development, optimizing printing techniques, and focusing on sustainability, the construction sector can achieve significant environmental and economic benefits. The transition towards greener and more sustainable construction practices, driven by advancements in 3D printing, is not only feasible but imperative for the future of the built environment.

Author Contributions: Conceptualization, Y.T. and İ.H.T.; methodology, Y.T., İ.H.T. and R.Ş.; validation, Y.T. and İ.H.T.; formal analysis, Y.T. and İ.H.T.; investigation, Y.T. and İ.H.T.; resources, Y.T. and İ.H.T.; data curation, Y.T. and İ.H.T.; writing—original draft preparation, Y.T. and İ.H.T.; writing—review and editing, Y.T., İ.H.T. and R.Ş.; visualization, Y.T. and İ.H.T.; supervision, R.Ş. All authors have read and agreed to the published version of the manuscript.

Funding: This research received no external funding.

Data Availability Statement: The original contributions presented in this study are included in the article; further inquiries can be directed to the corresponding author.

Conflicts of Interest: The authors declare no conflicts of interest.

References

1. Li, Y.; Zhang, H.; Zhang, Z.; Li, Y.; Fang, H.; Yuan, J.; Tang, S. The Early-Age Cracking Sensitivity, Shrinkage, Hydration Process, Pore Structure and Micromechanics of Cement-Based Materials Containing Alkalis with Different Metal Ions. *Dev. Built Environ.* **2024**, *18*, 100454. [CrossRef]
2. Feng, W.; Li, Z.; Long, Q.; Tang, S.; Zhao, Y. Study on the Properties of Autoclaved Aerated Concrete with High Content Concrete Slurry Waste. *Dev. Built Environ.* **2024**, *17*, 100338. [CrossRef]
3. Wangler, T.; Lloret, E.; Reiter, L.; Hack, N.; Gramazio, F.; Kohler, M.; Bernhard, M.; Dillenburger, B.; Buchli, J.; Roussel, N.; et al. Digital Concrete: Opportunities and Challenges. *RILEM Tech. Lett.* **2016**, *1*, 67–75. [CrossRef]
4. Paul, S.C.; Tay, Y.W.D.; Panda, B.; Tan, M.J. Fresh and Hardened Properties of 3D Printable Cementitious Materials for Building and Construction. *Arch. Civil. Mech. Eng.* **2018**, *18*, 311–319. [CrossRef]
5. Wi, K.; Suresh, V.; Wang, K.; Li, B.; Qin, H. Quantifying Quality of 3D Printed Clay Objects Using a 3D Structured Light Scanning System. *Addit. Manuf.* **2020**, *32*, 100987. [CrossRef]
6. Bock, T. The Future of Construction Automation: Technological Disruption and the Upcoming Ubiquity of Robotics. *Autom. Constr.* **2015**, *59*, 113–121. [CrossRef]
7. Alaloul, W.S.; Liew, M.S.; Zawawi, N.A.W.A.; Mohammed, B.S. Industry Revolution IR 4.0: Future Opportunities and Challenges in Construction Industry. *MATEC Web Conf.* **2018**, *203*, 02010. [CrossRef]
8. Craveiro, F.; Duarte, J.P.; Bartolo, H.; Bartolo, P.J. Additive Manufacturing as an Enabling Technology for Digital Construction: A Perspective on Construction 4.0. *Autom. Constr.* **2019**, *103*, 251–267. [CrossRef]
9. Zhang, Z.; Demir, K.G.; Gu, G.X. Developments in 4D-Printing: A Review on Current Smart Materials, Technologies, and Applications. *Int. J. Smart Nano Mater.* **2019**, *10*, 205–224. [CrossRef]
10. Craveiro, F.; Duarte, J.P.; Bártolo, H.; Bártolo, P. Moving Forward to 3D/4D Printed Building Facades. In *Progress in Digital and Physical Manufacturing*; Lecture Notes in Mechanical Engineering; Springer: Cham, Switzerland, 2020; pp. 277–282. [CrossRef]
11. Mogale, S.P. 3D Concrete Printing Technology: Enhancing Productivity in the South African Construction Industry-Exploring the Benefits, Barriers, and Improvement Strategies. Master's Thesis, Stellenbosch University, Stellenbosch, South Africa, 2023.
12. Jadhav, A.; Jadhav, V.S. A Review on 3D Printing: An Additive Manufacturing Technology. *Mater. Today Proc.* **2022**, *62*, 2094–2099. [CrossRef]
13. Tu, H.; Wei, Z.; Bahrami, A.; Ben Kahla, N.; Ahmad, A.; Özkılıç, Y.O. Recent Advancements and Future Trends in 3D Concrete Printing Using Waste Materials. *Dev. Built Environ.* **2023**, *16*, 100187. [CrossRef]
14. Nodehi, M.; Aguayo, F.; Nodehi, S.E.; Gholampour, A.; Ozbakkaloglu, T.; Gencel, O. Durability Properties of 3D Printed Concrete (3DPC). *Autom. Constr.* **2022**, *142*, 104479. [CrossRef]
15. Akman, A.; Sadhu, A. Recent Development of 3D-Printing Technology in Construction Engineering. *Pract. Period. Struct. Des. Constr.* **2023**, *29*, 03123005. [CrossRef]
16. Ngo, T.D.; Kashani, A.; Imbalzano, G.; Nguyen, K.T.Q.; Hui, D. Additive Manufacturing (3D Printing): A Review of Materials, Methods, Applications and Challenges. *Compos. B Eng.* **2018**, *143*, 172–196. [CrossRef]
17. Rehman, A.U.; Kim, J.H. 3D Concrete Printing: A Systematic Review of Rheology, Mix Designs, Mechanical, Microstructural, and Durability Characteristics. *Materials* **2021**, *14*, 3800. [CrossRef] [PubMed]
18. El-Sayegh, S.; Romdhane, L.; Manjikian, S. A Critical Review of 3D Printing in Construction: Benefits, Challenges, and Risks. *Arch. Civil. Mech. Eng.* **2020**, *20*, 34. [CrossRef]
19. Praveena, B.A.; Lokesh, N.; Buradi, A.; Santhosh, N.; Praveena, B.L.; Vignesh, R. A Comprehensive Review of Emerging Additive Manufacturing (3D Printing Technology): Methods, Materials, Applications, Challenges, Trends and Future Potential. *Mater. Today Proc.* **2022**, *52*, 1309–1313. [CrossRef]
20. Tarhan, Y.; Şahin, R. Fresh and Rheological Performances of Air-Entrained 3D Printable Mortars. *Materials* **2021**, *14*, 2409. [CrossRef] [PubMed]

21. Takagishi, K.; Umezu, S. Development of the Improving Process for the 3D Printed Structure. *Sci. Rep.* **2017**, *7*, 39852. [CrossRef] [PubMed]
22. Shah, J.; Snider, B.; Clarke, T.; Kozutsky, S.; Lacki, M.; Hosseini, A. Large-Scale 3D Printers for Additive Manufacturing: Design Considerations and Challenges. *Int. J. Adv. Manuf. Technol.* **2019**, *104*, 3679–3693. [CrossRef]
23. Žujović, M.; Obradović, R.; Rakonjac, I.; Milošević, J. 3D Printing Technologies in Architectural Design and Construction: A Systematic Literature Review. *Buildings* **2022**, *12*, 1319. [CrossRef]
24. Tarhan, Y.; Craveiro, F.; Bartolo, H. An Overview of Binder Materials' Sustainability for 3D Printing in Construction. In *Progress in Digital and Physical Manufacturing*; Springer: Cham, Switzerland, 2023; pp. 291–302. [CrossRef]
25. Lu, B.; Zhu, W.; Weng, Y.; Liu, Z.; Yang, E.H.; Leong, K.F.; Tan, M.J.; Wong, T.N.; Qian, S. Study of MgO-Activated Slag as a Cementless Material for Sustainable Spray-Based 3D Printing. *J. Clean. Prod.* **2020**, *258*, 120671. [CrossRef]
26. Singh, N.; Colangelo, F.; Farina, I. Sustainable Non-Conventional Concrete 3D Printing—A Review. *Sustainability* **2023**, *15*, 10121. [CrossRef]
27. Rudziewicz, M.; Maroszek, M.; Góra, M.; Dziura, P.; Mróz, K.; Hager, I.; Hebda, M. Feasibility Review of Aerated Materials Application in 3D Concrete Printing. *Materials* **2023**, *16*, 6032. [CrossRef]
28. Al-Tamimi, A.K.; Alqamish, H.H.; Khaldoune, A.; Alhaidary, H.; Shirvanimoghaddam, K. Framework of 3D Concrete Printing Potential and Challenges. *Buildings* **2023**, *13*, 827. [CrossRef]
29. Motalebi, A.; Khondoker, M.A.H.; Kabir, G. A Systematic Review of Life Cycle Assessments of 3D Concrete Printing. *Sustain. Oper. Comput.* **2024**, *5*, 41–50. [CrossRef]
30. Khajavi, S.H.; Tetik, M.; Mohite, A.; Peltokorpi, A.; Li, M.; Weng, Y.; Holmström, J. Additive Manufacturing in the Construction Industry: The Comparative Competitiveness of 3D Concrete Printing. *Appl. Sci.* **2021**, *11*, 3865. [CrossRef]
31. Batikha, M.; Jotangia, R.; Baaj, M.Y.; Mousleh, I. 3D Concrete Printing for Sustainable and Economical Construction: A Comparative Study. *Autom. Constr.* **2022**, *134*, 104087. [CrossRef]
32. Bhattacherjee, S.; Basavaraj, A.S.; Rahul, A.V.; Santhanam, M.; Gettu, R.; Panda, B.; Schlangen, E.; Chen, Y.; Copuroglu, O.; Ma, G.; et al. Sustainable Materials for 3D Concrete Printing. *Cem. Concr. Compos.* **2021**, *122*, 104156. [CrossRef]
33. Anonymous. THE 17 GOALS | Sustainable Development. Available online: https://sdgs.un.org/goals (accessed on 15 May 2024).
34. De Schutter, G.; Lesage, K.; Mechtcherine, V.; Nerella, V.N.; Habert, G.; Agusti-Juan, I. Vision of 3D Printing with Concrete—Technical, Economic and Environmental Potentials. *Cem. Concr. Res.* **2018**, *112*, 25–36. [CrossRef]
35. Markin, V.; Nerella, V.N.; Schröfl, C.; Guseynova, G.; Mechtcherine, V. Material Design and Performance Evaluation of Foam Concrete for Digital Fabrication. *Materials* **2019**, *12*, 2433. [CrossRef]
36. Le, T.T.; Austin, S.A.; Lim, S.; Buswell, R.A.; Law, R.; Gibb, A.G.F.; Thorpe, T. Hardened Properties of High-Performance Printing Concrete. *Cem. Concr. Res.* **2012**, *42*, 558–566. [CrossRef]
37. Rückrich, S.; Agranati, G.; Grobman, Y.J. Earth-Based Additive Manufacturing: A Field-Oriented Methodology for Evaluating Material Printability. *Archit. Sci. Rev.* **2023**, *66*, 133–143. [CrossRef]
38. Ahmed, G.H.; Askandar, N.H.; Jumaa, G.B. A Review of Largescale 3DCP: Material Characteristics, Mix Design, Printing Process, and Reinforcement Strategies. *Structures* **2022**, *43*, 508–532. [CrossRef]
39. Nair, A.; Aditya, S.D.; Adarsh, R.N.; Nandan, M.; Dharek, M.S.; Sreedhara, B.M.; Prashant, S.C.; Sreekeshava, K.S. Additive Manufacturing of Concrete: Challenges and Opportunities. *IOP Conf. Ser. Mater. Sci. Eng.* **2020**, *814*, 012022. [CrossRef]
40. Zhang, Y.; Zhang, Y.; She, W.; Yang, L.; Liu, G.; Yang, Y. Rheological and Harden Properties of the High-Thixotropy 3D Printing Concrete. *Constr. Build. Mater.* **2019**, *201*, 278–285. [CrossRef]
41. Dilawar Riaz, R.; Usman, M.; Ali, A.; Majid, U.; Faizan, M.; Jalil Malik, U. Inclusive Characterization of 3D Printed Concrete (3DPC) in Additive Manufacturing: A Detailed Review. *Constr. Build. Mater.* **2023**, *394*, 132229. [CrossRef]
42. Le, T.T.; Austin, S.A.; Lim, S.; Buswell, R.A.; Gibb, A.G.F.; Thorpe, T. Mix Design and Fresh Properties for High-Performance Printing Concrete. *Mater. Struct. /Mater. et Constr.* **2012**, *45*, 1221–1232. [CrossRef]
43. Tarhan, Y.; Şahin, R. Developments of 3D concrete printing process. In Proceedings of the International Civil Engineering & Architecture Conference, Trabzon, Turkey, 17–20 April 2019; pp. 2394–2404.
44. Weng, Y.; Lu, B.; Li, M.; Liu, Z.; Tan, M.J.; Qian, S. Empirical Models to Predict Rheological Properties of Fiber Reinforced Cementitious Composites for 3D Printing. *Constr. Build. Mater.* **2018**, *189*, 676–685. [CrossRef]
45. Roussel, N. Rheological Requirements for Printable Concretes. *Cem. Concr. Res.* **2018**, *112*, 76–85. [CrossRef]
46. Yang, E.-H.; Sahmaran, M.; Yang, Y.; Li, V.C. Rheological Control in Production of Engineered Cementitious Composites. *ACI Mater. J.* **2009**, *106*, 357. [CrossRef]
47. Wi, K.; Wang, K.; Taylor, P.C.; Laflamme, S.; Sritharan, S.; Qin, H. Properties and Microstructure of Extrusion-Based 3D Printing Mortar Containing a Highly Flowable, Rapid Set Grout. *Cem. Concr. Compos.* **2021**, *124*, 104243. [CrossRef]

48. Antoni, A.; Adi, N.; Kurniawan, M.E.; Agraputra, A.; Teopilus, D.; Pudjisuryadi, P.; Chandra, J.; Hardjito, D. The Influence of Viscosity-Modifying Agent and Calcium Carbonate on 3D Printing Mortar Characteristics. *IOP Conf. Ser. Earth Environ. Sci.* **2023**, *1195*, 012021. [CrossRef]
49. Zaid, O.; El Ouni, M.H. Advancements in 3D Printing of Cementitious Materials: A Review of Mineral Additives, Properties, and Systematic Developments. *Constr. Build. Mater.* **2024**, *427*, 136254. [CrossRef]
50. Ma, G.; Li, Z.; Wang, L. Printable Properties of Cementitious Material Containing Copper Tailings for Extrusion Based 3D Printing. *Constr. Build. Mater.* **2018**, *162*, 613–627. [CrossRef]
51. Moeini, M.A.; Hosseinpoor, M.; Yahia, A. Use of the Chemical and Mineral Admixtures to Tailor the Rheology and the Green Strength of 3D Printing Cementitious Mixtures. *RILEM Bookseries* **2020**, *28*, 73–82. [CrossRef]
52. Said, F.; Eldwib, D.; Zaytoun, M.; Abd Elsalam, A.; Bakhoum, M.; Elshehemy, O.; Abou Ali, R.; El-Gamal, S.; Abou-Zeid, M. 3D Printing Concrete Incoroprating Environmentally Friendly Materials. *Lect. Notes Civil. Eng.* **2023**, *248*, 627–639. [CrossRef]
53. Volpe, S.; Sangiorgio, V.; Petrella, A.; Coppola, A.; Notarnicola, M.; Fiorito, F. Building Envelope Prefabricated with 3D Printing Technology. *Sustainability* **2021**, *13*, 8923. [CrossRef]
54. Zhang, Y.; Zhang, Y.; Liu, G.; Yang, Y.; Wu, M.; Pang, B. Fresh Properties of a Novel 3D Printing Concrete Ink. *Constr. Build. Mater.* **2018**, *174*, 263–271. [CrossRef]
55. Papachristoforou, M.; Mitsopoulos, V.; Stefanidou, M. Evaluation of Workability Parameters in 3D Printing Concrete. *Procedia Struct. Integr.* **2018**, *10*, 155–162. [CrossRef]
56. Dai, P.; Lyu, Q.; Zong, M.; Zhu, P. Effect of Waste Plastic Fibers on the Printability and Mechanical Properties of 3D-Printed Cement Mortar. *J. Build. Eng.* **2024**, *83*, 108439. [CrossRef]
57. Statkauskas, M.; Grinys, A.; Vaičiukynienė, D. Investigation of Concrete Shrinkage Reducing Additives. *Materials* **2022**, *15*, 3407. [CrossRef] [PubMed]
58. Jiang, Q.; Liu, Q.; Wu, S.; Zheng, H.; Sun, W. Modification Effect of Nanosilica and Polypropylene Fiber for Extrusion-Based 3D Printing Concrete: Printability and Mechanical Anisotropy. *Addit. Manuf.* **2022**, *56*, 102944. [CrossRef]
59. Chao, Y.; Zhang, H.; Li, J.; Duong, T.Q.; Korolev, E.; Inozemtcev, A. Selection of Reinforcing Fiber for High-Strength Lightweight Concrete for 3D-Printing. *IOP Conf. Ser. Mater. Sci. Eng.* **2021**, *1030*, 012007. [CrossRef]
60. Marczyk, J.; Ziejewska, C.; Gadek, S.; Korniejenko, K.; Łach, M.; Góra, M.; Kurek, I.; Dogan-Saglamtimur, N.; Hebda, M.; Szechynska-Hebda, M. Hybrid Materials Based on Fly Ash, Metakaolin, and Cement for 3d Printing. *Materials* **2021**, *14*, 6874. [CrossRef]
61. Chougan, M.; Hamidreza Ghaffar, S.; Nematollahi, B.; Sikora, P.; Dorn, T.; Stephan, D.; Albar, A.; Al-Kheetan, M.J. Effect of Natural and Calcined Halloysite Clay Minerals as Low-Cost Additives on the Performance of 3D-Printed Alkali-Activated Materials. *Mater. Des.* **2022**, *223*, 111183. [CrossRef]
62. Ding, T.; Xiao, J.; Zou, S.; Wang, Y. Hardened Properties of Layered 3D Printed Concrete with Recycled Sand. *Cem. Concr. Compos.* **2020**, *113*, 103724. [CrossRef]
63. Muthukrishnan, S.; Kua, H.W.; Yu, L.N.; Chung, J.K.H. Fresh Properties of Cementitious Materials Containing Rice Husk Ash for Construction 3D Printing. *J. Mater. Civil. Eng.* **2020**, *32*, 04020195. [CrossRef]
64. Bos, F.P.; Kruger, P.J.; Lucas, S.S.; van Zijl, G.P.A.G. Juxtaposing Fresh Material Characterisation Methods for Buildability Assessment of 3D Printable Cementitious Mortars. *Cem. Concr. Compos.* **2021**, *120*, 104024. [CrossRef]
65. Rahul, A.V.; Sharma, A.; Santhanam, M. A Desorptivity-Based Approach for the Assessment of Phase Separation during Extrusion of Cementitious Materials. *Cem. Concr. Compos.* **2020**, *108*, 103546. [CrossRef]
66. Kazemian, A.; Yuan, X.; Meier, R.; Khoshnevis, B. Performance-Based Testing of Portland Cement Concrete for Construction-Scale 3D Printing. *3d Concr. Print. Technol. Constr. Build. Appl.* **2019**, 13–35. [CrossRef]
67. Hambach, M.; Rutzen, M.; Volkmer, D. Properties of 3D-Printed Fiber-Reinforced Portland Cement Paste. *3d Concr. Print. Technol. Constr. Build. Appl.* **2019**, 73–113. [CrossRef]
68. Perrot, A.; Rangeard, D.; Pierre, A. Structural Built-up of Cement-Based Materials Used for 3D-Printing Extrusion Techniques. *Mater. Struct./Mater. et Constr.* **2016**, *49*, 1213–1220. [CrossRef]
69. Ibrahim, K.A.; Van Zijl, G.P.A.G.; Babafemi, A.J. Influence of Limestone Calcined Clay Cement on Properties of 3D Printed Concrete for Sustainable Construction. *J. Build. Eng.* **2023**, *69*, 2352–7102. [CrossRef]
70. Qiu, M.; Sun, Y.; Qian, Y. Interfacial Bonding Performance of 3D-Printed Ultra-High Performance Strain-Hardening Cementitious Composites (UHP-SHCC) and Cast Normal Concrete. *J. Build. Eng.* **2024**, *82*, 108268. [CrossRef]
71. Singh, A.; Wang, Y.; Zhou, Y.; Sun, J.; Xu, X.; Li, Y.; Liu, Z.; Chen, J.; Wang, X. Utilization of Antimony Tailings in Fiber-Reinforced 3D Printed Concrete: A Sustainable Approach for Construction Materials. *Constr. Build. Mater.* **2023**, *408*, 133689. [CrossRef]
72. Lucen, H.; Long, L.; Shipeng, Z.; Huanghua, Z.; Jianzhuang, X.; Chi Sun, P. The Synergistic Effect of Greenhouse Gas CO_2 and Silica Fume on the Properties of 3D Printed Mortar. *Compos. B Eng.* **2024**, *271*, 111188. [CrossRef]
73. Teh, S.H.; Wiedmann, T.; Castel, A.; de Burgh, J. Hybrid Life Cycle Assessment of Greenhouse Gas Emissions from Cement, Concrete and Geopolymer Concrete in Australia. *J. Clean. Prod.* **2017**, *152*, 312–320. [CrossRef]

74. Zhang, C.; Nerella, V.N.; Krishna, A.; Wang, S.; Zhang, Y.; Mechtcherine, V.; Banthia, N. Mix Design Concepts for 3D Printable Concrete: A Review. *Cem. Concr. Compos.* **2021**, *122*, 104155. [CrossRef]
75. Zhang, X.; Heeren, N.; Bauer, C.; Burgherr, P.; McKenna, R.; Habert, G. The Impacts of Future Sectoral Change on the Greenhouse Gas Emissions of Construction Materials for Swiss Residential Buildings. *Energy Build.* **2024**, *303*, 113824. [CrossRef]
76. Mohamad, N.; Muthusamy, K.; Embong, R.; Kusbiantoro, A.; Hashim, M.H. Environmental Impact of Cement Production and Solutions: A Review. *Mater. Today Proc.* **2022**, *48*, 741–746. [CrossRef]
77. Barbhuiya, S.; Bhusan Das, B.; Adak, D. Roadmap to a Net-Zero Carbon Cement Sector: Strategies, Innovations and Policy Imperatives. *J. Environ. Manag.* **2024**, *359*, 121052. [CrossRef]
78. Cavalett, O.; Watanabe, M.D.B.; Voldsund, M.; Roussanaly, S.; Cherubini, F. Paving the Way for Sustainable Decarbonization of the European Cement Industry. *Nat. Sustain.* **2024**, *7*, 568–580. [CrossRef]
79. Barbhuiya, S.; Kanavaris, F.; Das, B.B.; Idrees, M. Decarbonising Cement and Concrete Production: Strategies, Challenges and Pathways for Sustainable Development. *J. Build. Eng.* **2024**, *86*, 108861. [CrossRef]
80. Griffiths, S.; Sovacool, B.K.; Furszyfer Del Rio, D.D.; Foley, A.M.; Bazilian, M.D.; Kim, J.; Uratani, J.M. Decarbonizing the Cement and Concrete Industry: A Systematic Review of Socio-Technical Systems, Technological Innovations, and Policy Options. *Renew. Sustain. Energy Rev.* **2023**, *180*, 113291. [CrossRef]
81. Jotangia, R.; Batikha, M. Heriot-Watt University's Centre of Excellence in Smart Construction Research Bulletin. Heriot-Watt University: Edinburgh, UK, 2021; pp. 31–35.
82. Tonelli, M.; Faralli, A.; Ridi, F.; Bonini, M. 3D Printable Magnesium-Based Cements towards the Preparation of Bioceramics. *J. Colloid. Interface Sci.* **2021**, *598*, 24–35. [CrossRef] [PubMed]
83. Panda, B.; Sonat, C.; Yang, E.H.; Tan, M.J.; Unluer, C. Use of Magnesium-Silicate-Hydrate (M-S-H) Cement Mixes in 3D Printing Applications. *Cem. Concr. Compos.* **2021**, *117*, 103901. [CrossRef]
84. Tayyab, A.; Kienzle, A.; Thomas, R.J. Engineering Properties and Setting Time of Belitic Calcium Sulfoaluminate (BCSA) Cement Concrete. *Constr. Build. Mater.* **2022**, *352*, 128979. [CrossRef]
85. Olajire, A.A. A Review of Mineral Carbonation Technology in Sequestration of CO_2. *J. Pet. Sci. Eng.* **2013**, *109*, 364–392. [CrossRef]
86. Pasupathy, K.; Ramakrishnan, S.; Sanjayan, J. 3D Concrete Printing of Eco-Friendly Geopolymer Containing Brick Waste. *Cem. Concr. Compos.* **2023**, *138*, 104943. [CrossRef]
87. Reddy, M.S.; Dinakar, P.; Rao, B.H. Mix Design Development of Fly Ash and Ground Granulated Blast Furnace Slag Based Geopolymer Concrete. *J. Build. Eng.* **2018**, *20*, 712–722. [CrossRef]
88. Khalil, N.; Aouad, G.; El Cheikh, K.; Rémond, S. Use of Calcium Sulfoaluminate Cements for Setting Control of 3D-Printing Mortars. *Constr. Build. Mater.* **2017**, *157*, 382–391. [CrossRef]
89. Abu-Ennab, L.; Dixit, M.K.; Birgisson, B.; Pradeep Kumar, P. Comparative Life Cycle Assessment of Large-Scale 3D Printing Utilizing Kaolinite-Based Calcium Sulfoaluminate Cement Concrete and Conventional Construction. *Clean. Environ. Syst.* **2022**, *5*, 100078. [CrossRef]
90. de Matos, P.R.; Zat, T.; Lima, M.M.; Andrade Neto, J.d.S.; Souza, M.T.; Rodríguez, E.D. Effect of the Superplasticizer Addition Time on the Fresh Properties of 3D Printed Limestone Calcined Clay Cement (LC3) Concrete. *Case Stud. Constr. Mater.* **2023**, *19*, e02419. [CrossRef]
91. Wang, X.; Krishnan, P.; Celik, K. Enhancing Carbonation and Thermal Insulation of Reactive Magnesium Oxide Cement (RMC)-Based 3D Printable Pastes with Cenospheres. *Cem. Concr. Compos.* **2024**, *150*, 105559. [CrossRef]
92. Khalil, A.; Wang, X.; Celik, K. 3D Printable Magnesium Oxide Concrete: Towards Sustainable Modern Architecture. *Addit. Manuf.* **2020**, *33*, 101145. [CrossRef]
93. Liao, Y.; Cai, Z.; Deng, F.; Ye, J.; Wang, K.; Tang, S. Hydration Behavior and Thermodynamic Modelling of Ferroaluminate Cement Blended with Steel Slag. *J. Build. Eng.* **2024**, *97*, 110833. [CrossRef]
94. Scrivener, K.L.; John, V.M.; Gartner, E.M. Eco-Efficient Cements: Potential Economically Viable Solutions for a Low-CO2 Cement-Based Materials Industry. *Cem. Concr. Res.* **2018**, *114*, 2–26. [CrossRef]
95. Chaunsali, P.; Mondal, P. Influence of Calcium Sulfoaluminate (CSA) Cement Content on Expansion and Hydration Behavior of Various Ordinary Portland Cement-CSA Blends. *J. Am. Ceram. Soc.* **2015**, *98*, 2617–2624. [CrossRef]
96. Chaunsali, P.; Ardeshirilajimi, A.; Mondal, P. On the Interaction of Class C Fly Ash with Portland Cement–Calcium Sulfoaluminate Cement Binder. *Mater. Struct./Mater. et Constr.* **2018**, *51*, 1–9. [CrossRef]
97. Mohan, M.K.; Rahul, A.V.; De Schutter, G.; Van Tittelboom, K. Early Age Hydration, Rheology and Pumping Characteristics of CSA Cement-Based 3D Printable Concrete. *Constr. Build. Mater.* **2021**, *275*, 122136. [CrossRef]
98. Afroughsabet, V.; Biolzi, L.; Monteiro, P.J.M.; Gastaldi, M.M. Investigation of the Mechanical and Durability Properties of Sustainable High Performance Concrete Based on Calcium Sulfoaluminate Cement. *J. Build. Eng.* **2021**, *43*, 102656. [CrossRef]
99. Zhu, J.; Zhang, T.; Faried, M.; Chen, W. 3D Printing Cement Based Ink, and It's Application within the Construction Industry. *MATEC Web Conf.* **2017**, *120*, 02003. [CrossRef]

100. Xu, Z.; Zhang, D.; Li, H.; Sun, X.; Zhao, K.; Wang, Y. Effect of FA and GGBFS on Compressive Strength, Rheology, and Printing Properties of Cement-Based 3D Printing Material. *Constr. Build. Mater.* **2022**, *339*, 127685. [CrossRef]
101. Rubio, M.; Sonebi, M.; Amziane, S. 3D Printing of Fibre Cement-Based Materials: Fresh and Rheological Performances. *Acad. J. Civil. Eng.* **2017**, *35*, 480–488. [CrossRef]
102. Yuan, Q.; Li, Z.; Zhou, D.; Huang, T.; Huang, H.; Jiao, D.; Shi, C. A Feasible Method for Measuring the Buildability of Fresh 3D Printing Mortar. *Constr. Build. Mater.* **2019**, *227*, 116600. [CrossRef]
103. Kruger, J.; Zeranka, S.; van Zijl, G. A Rheology-Based Quasi-Static Shape Retention Model for Digitally Fabricated Concrete. *Constr. Build. Mater.* **2020**, *254*, 119241. [CrossRef]
104. Kruger, J.; Zeranka, S.; van Zijl, G. An Ab Initio Approach for Thixotropy Characterisation of (Nanoparticle-Infused) 3D Printable Concrete. *Constr. Build. Mater.* **2019**, *224*, 372–386. [CrossRef]
105. Lee, K.-W.; Lee, H.-J.; Choi, M.-S. Correlation between Thixotropic Behavior and Buildability for 3D Concrete Printing. *Constr. Build. Mater.* **2022**, *347*, 128498. [CrossRef]
106. Weng, Y.; Li, M.; Tan, M.J.; Qian, S. Design 3D Printing Cementitious Materials via Fuller Thompson Theory and Marson-Percy Model. *Constr. Build. Mater.* **2018**, *163*, 600–610. [CrossRef]
107. Zhang, C.; Hou, Z.; Chen, C.; Zhang, Y.; Mechtcherine, V.; Sun, Z. Design of 3D Printable Concrete Based on the Relationship between Flowability of Cement Paste and Optimum Aggregate Content. *Cem. Concr. Compos.* **2019**, *104*, 103406. [CrossRef]
108. Moeini, M.A.; Hosseinpoor, M.; Yahia, A. Effectiveness of the Rheometric Methods to Evaluate the Build-up of Cementitious Mortars Used for 3D Printing. *Constr. Build. Mater.* **2020**, *257*, 119551. [CrossRef]
109. Qian, Y.; De Schutter, G. Enhancing Thixotropy of Fresh Cement Pastes with Nanoclay in Presence of Polycarboxylate Ether Superplasticizer (PCE). *Cem. Concr. Res.* **2018**, *111*, 15–22. [CrossRef]
110. Panda, B.; Lim, J.H.; Tan, M.J. Mechanical Properties and Deformation Behaviour of Early Age Concrete in the Context of Digital Construction. *Compos. B Eng.* **2019**, *165*, 563–571. [CrossRef]
111. Harbouz, I.; Roziere, E.; Yahia, A.; Loukili, A. Printability Assessment of Cement-Based Materials Based on Rheology, Hydration Kinetics, and Viscoelastic Properties. *Constr. Build. Mater.* **2022**, *325*, 126810. [CrossRef]
112. Mohan, M.K.; Rahul, A.V.; Van Tittelboom, K.; De Schutter, G. Rheological and Pumping Behaviour of 3D Printable Cementitious Materials with Varying Aggregate Content. *Cem. Concr. Res.* **2021**, *139*, 106258. [CrossRef]
113. Chen, M.; Liu, B.; Li, L.; Cao, L.; Huang, Y.; Wang, S.; Zhao, P.; Lu, L.; Cheng, X. Rheological Parameters, Thixotropy and Creep of 3D-Printed Calcium Sulfoaluminate Cement Composites Modified by Bentonite. *Compos. B Eng.* **2020**, *186*, 107821. [CrossRef]
114. Long, W.-J.; Tao, J.-L.; Lin, C.; Gu, Y.; Mei, L.; Duan, H.-B.; Xing, F. Rheology and Buildability of Sustainable Cement-Based Composites Containing Micro-Crystalline Cellulose for 3D-Printing. *J. Clean. Prod.* **2019**, *239*, 118054. [CrossRef]
115. Tran, M.V.; Cu, Y.T.H.; Le, C.V.H. Rheology and Shrinkage of Concrete Using Polypropylene Fiber for 3D Concrete Printing. *J. Build. Eng.* **2021**, *44*, 103400. [CrossRef]
116. Tramontin Souza, M.; Maia Ferreira, I.; Guzi de Moraes, E.; Senff, L.; Arcaro, S.; Castro Pessôa, J.R.; J. Ribeiro, M.; Novaes de Oliveira, A.P. Role of Chemical Admixtures on 3D Printed Portland Cement: Assessing Rheology and Buildability. *Constr. Build. Mater.* **2022**, *314*, 125666. [CrossRef]
117. Nerella, V.N.; Beigh, M.A.B.; Fataei, S.; Mechtcherine, V. Strain-Based Approach for Measuring Structural Build-up of Cement Pastes in the Context of Digital Construction. *Cem. Concr. Res.* **2019**, *115*, 530–544. [CrossRef]
118. Prevedello Rubin, A.; Hasse, J.A.; Longuini Repette, W. The Evaluation of Rheological Parameters of 3D Printable Concretes and the Effect of Accelerating Admixture. *Constr. Build. Mater.* **2021**, *276*, 122221. [CrossRef]
119. Chen, M.; Yang, L.; Zheng, Y.; Huang, Y.; Li, L.; Zhao, P.; Wang, S.; Lu, L.; Cheng, X. Yield Stress and Thixotropy Control of 3D-Printed Calcium Sulfoaluminate Cement Composites with Metakaolin Related to Structural Build-Up. *Constr. Build. Mater.* **2020**, *252*, 119090. [CrossRef]
120. Jayathilakage, R.; Rajeev, P.; Sanjayan, J.G. Yield Stress Criteria to Assess the Buildability of 3D Concrete Printing. *Constr. Build. Mater.* **2020**, *240*, 117989. [CrossRef]
121. Singh, N.B.; Middendorf, B. Geopolymers as an Alternative to Portland Cement: An Overview. *Constr. Build. Mater.* **2020**, *237*, 117455. [CrossRef]
122. Panda, B.; Paul, S.C.; Hui, L.J.; Tay, Y.W.D.; Tan, M.J. Additive Manufacturing of Geopolymer for Sustainable Built Environment. *J. Clean. Prod.* **2017**, *167*, 281–288. [CrossRef]
123. Davidovits, J. Geopolymers: Inorganic Polymeric New Materials. *J. Therm. Anal. Calorim.* **2005**, *37*, 1633–1656. [CrossRef]
124. Zhao, J.; Tong, L.; Li, B.; Chen, T.; Wang, C.; Yang, G.; Zheng, Y. Eco-Friendly Geopolymer Materials: A Review of Performance Improvement, Potential Application and Sustainability Assessment. *J. Clean. Prod.* **2021**, *307*, 127085. [CrossRef]
125. Singh, B.; Ishwarya, G.; Gupta, M.; Bhattacharyya, S.K. Geopolymer Concrete: A Review of Some Recent Developments. *Constr. Build. Mater.* **2015**, *85*, 78–90. [CrossRef]
126. Hassan, A.; Arif, M.; Shariq, M. A Review of Properties and Behaviour of Reinforced Geopolymer Concrete Structural Elements-A Clean Technology Option for Sustainable Development. *J. Clean. Prod.* **2020**, *245*, 118762. [CrossRef]

127. Kumar, M.L.; Revathi, V. Microstructural Properties of Alkali-Activated Metakaolin and Bottom Ash Geopolymer. *Arab. J. Sci. Eng.* **2020**, *45*, 4235–4246. [CrossRef]
128. Nagalia, G.; Park, Y.; Abolmaali, A.; Aswath, P. Compressive Strength and Microstructural Properties of Fly Ash–Based Geopolymer Concrete. *J. Mater. Civil. Eng.* **2016**, *28*, 04016144. [CrossRef]
129. Badrawi, H.A.; Makahleh, H.Y.; Haweileh, R.A. Compressive Strength and Durability of Geopolymer Concrete. In Proceedings of the 2022 Advances in Science and Engineering Technology International Conferences, ASET 2022, Dubai, United Arab Emirates, 21–24 February 2022. [CrossRef]
130. Pilehvar, S.; Szczotok, A.M.; Rodríguez, J.F.; Valentini, L.; Lanzón, M.; Pamies, R.; Kjøniksen, A.L. Effect of Freeze-Thaw Cycles on the Mechanical Behavior of Geopolymer Concrete and Portland Cement Concrete Containing Micro-Encapsulated Phase Change Materials. *Constr. Build. Mater.* **2019**, *200*, 94–103. [CrossRef]
131. Neupane, K.; Chalmers, D.; Kidd, P. High-Strength Geopolymer Concrete- Properties, Advantages and Challenges. *Adv. Mater.* **2018**, *7*, 15–25. [CrossRef]
132. Antoni, A.; Purwantoro, A.A.T.; Suyanto, W.S.P.D.; Hardjito, D. Fresh and Hardened Properties of High Calcium Fly Ash-Based Geopolymer Matrix with High Dosage of Borax. *Iran. J. Sci. Technol.—Trans. Civil. Eng.* **2020**, *44*, 535–543. [CrossRef]
133. Olivia, M.; Nikraz, H. Properties of Fly Ash Geopolymer Concrete Designed by Taguchi Method. *Mater. Des. (1980–2015)* **2012**, *36*, 191–198. [CrossRef]
134. Kleshchevnikova, V.; Belyaeva, S.; Baranov, A. Optimization of Mix Designs and Experimental Study of the Properties of Concrete Mix for 3D Printing. In Proceedings of the EECE 2020; Lecture Notes in Civil Engineering. Springer: Cham, Switzerland, 2021; Volume 150, pp. 151–160. [CrossRef]
135. Kurtoglu, A.E.; Alzeebaree, R.; Aljumaili, O.; Nis, A.; Gulsan, M.E.; Humur, G.; Cevik, A.; Kurtoglu, A.E.; Alzeebaree, R.; Aljumaili, O.; et al. Advances in Concrete Construction. *Adv. Concr. Constr.* **2018**, *6*, 345. [CrossRef]
136. Niveditha, M.; Koniki, S. Effect of Durability Properties on Geopolymer Concrete—A Review. *E3S Web Conf.* **2020**, *184*, 01092. [CrossRef]
137. Zhang, B. Durability of Low-Carbon Geopolymer Concrete: A Critical Review. *Sustain. Mater. Technol.* **2024**, *40*, e00882. [CrossRef]
138. Marczyk, J.; Ziejewska, C.; Korniejenko, K.; Łach, M.; Marzec, W.; Góra, M.; Dziura, P.; Sprince, A.; Szechyńska-Hebda, M.; Hebda, M. Properties of 3D Printed Concrete–Geopolymer Hybrids Reinforced with Aramid Roving. *Materials* **2022**, *15*, 6132. [CrossRef]
139. Jiang, X.; Xiao, R.; Zhang, M.; Hu, W.; Bai, Y.; Huang, B. A Laboratory Investigation of Steel to Fly Ash-Based Geopolymer Paste Bonding Behavior after Exposure to Elevated Temperatures. *Constr. Build. Mater.* **2020**, *254*, 119267. [CrossRef]
140. Luhar, S.; Luhar, I.; Gupta, R. Durability Performance Evaluation of Green Geopolymer Concrete. *Eur. J. Environ. Civil. Eng.* **2022**, *26*, 4297–4345. [CrossRef]
141. Noushini, A.; Castel, A. The Effect of Heat-Curing on Transport Properties of Low-Calcium Fly Ash-Based Geopolymer Concrete. *Constr. Build. Mater.* **2016**, *112*, 464–477. [CrossRef]
142. Castel, A.; Foster, S.J.; Ng, T.; Sanjayan, J.G.; Gilbert, R.I. Creep and Drying Shrinkage of a Blended Slag and Low Calcium Fly Ash Geopolymer Concrete. *Mater. Struct./Mater. et Constr.* **2016**, *49*, 1619–1628. [CrossRef]
143. Farooq, F.; Jin, X.; Faisal Javed, M.; Akbar, A.; Izhar Shah, M.; Aslam, F.; Alyousef, R. Geopolymer Concrete as Sustainable Material: A State of the Art Review. *Constr. Build. Mater.* **2021**, *306*, 124762. [CrossRef]
144. Assi, L.N.; Carter, K.; Deaver, E.; Ziehl, P. Review of Availability of Source Materials for Geopolymer/Sustainable Concrete. *J. Clean. Prod.* **2020**, *263*, 121477. [CrossRef]
145. Salas, D.A.; Ramirez, A.D.; Ulloa, N.; Baykara, H.; Boero, A.J. Life Cycle Assessment of Geopolymer Concrete. *Constr. Build. Mater.* **2018**, *190*, 170–177. [CrossRef]
146. Meng, Q.; Wu, C.; Hao, H.; Li, J.; Wu, P.; Yang, Y.; Wang, Z. Steel Fibre Reinforced Alkali-Activated Geopolymer Concrete Slabs Subjected to Natural Gas Explosion in Buried Utility Tunnel. *Constr. Build. Mater.* **2020**, *246*, 118447. [CrossRef]
147. Senff, L.; Novais, R.M.; Carvalheiras, J.; Labrincha, J.A. Eco-Friendly Approach to Enhance the Mechanical Performance of Geopolymer Foams: Using Glass Fibre Waste Coming from Wind Blade Production. *Constr. Build. Mater.* **2020**, *239*, 117805. [CrossRef]
148. Wongsa, A.; Kunthawatwong, R.; Naenudon, S.; Sata, V.; Chindaprasirt, P. Natural Fiber Reinforced High Calcium Fly Ash Geopolymer Mortar. *Constr. Build. Mater.* **2020**, *241*, 118143. [CrossRef]
149. Aygörmez, Y.; Canpolat, O.; Al-mashhadani, M.M.; Uysal, M. Elevated Temperature, Freezing-Thawing and Wetting-Drying Effects on Polypropylene Fiber Reinforced Metakaolin Based Geopolymer Composites. *Constr. Build. Mater.* **2020**, *235*, 117502. [CrossRef]
150. Anonymous. (Webpage RENCA). RENCA Makes History with World's First Geopolymer House—3Dnatives. Available online: https://www.3dnatives.com/en/renca-makes-history-with-worlds-first-geopolymer-house/ (accessed on 16 May 2024).
151. Panda, B.; Singh, G.B.; Unluer, C.; Tan, M.J. Synthesis and Characterization of One-Part Geopolymers for Extrusion Based 3D Concrete Printing. *J. Clean. Prod.* **2019**, *220*, 610–619. [CrossRef]

152. Xia, M.; Sanjayan, J. Method of Formulating Geopolymer for 3D Printing for Construction Applications. *Mater. Des.* **2016**, *110*, 382–390. [CrossRef]
153. Aldin, Z. *3D Printing of Geopolymer Concrete 2019*; Delft University of Technology: Delft, The Netherlands, 2019.
154. Lim, J.H.; Panda, B.; Pham, Q.C. Improving Flexural Characteristics of 3D Printed Geopolymer Composites with In-Process Steel Cable Reinforcement. *Constr. Build. Mater.* **2018**, *178*, 32–41. [CrossRef]
155. Ma, G.; Li, Z.; Wang, L.; Bai, G. Micro-Cable Reinforced Geopolymer Composite for Extrusion-Based 3D Printing. *Mater. Lett.* **2019**, *235*, 144–147. [CrossRef]
156. Li, Z.; Wang, L.; Ma, G. Mechanical Improvement of Continuous Steel Microcable Reinforced Geopolymer Composites for 3D Printing Subjected to Different Loading Conditions. *Compos. B Eng.* **2020**, *187*, 107796. [CrossRef]
157. Muthukrishnan, S.; Ramakrishnan, S.; Sanjayan, J. Effect of Alkali Reactions on the Rheology of One-Part 3D Printable Geopolymer Concrete. *Cem. Concr. Compos.* **2021**, *116*, 103899. [CrossRef]
158. Hojati, M.; Nazarian, S.; Duarte, J.; Ashrafi, N.; Duarte, J.P.; Radlińska, A.; Craveiro, F.; Bilén, S. 3D Printing of Concrete: A Continuous Exploration of Mix Design and Printing Process. In Proceedings of the 42nd IAHS World Congress on Housing, Naples, Italy, 10–13 April 2018.
159. Panda, B.; Ruan, S.; Unluer, C.; Tan, M.J. Investigation of the Properties of Alkali-Activated Slag Mixes Involving the Use of Nanoclay and Nucleation Seeds for 3D Printing. *Compos. B Eng.* **2020**, *186*, 107826. [CrossRef]
160. Santana, H.A.; Neto, J.S.A.; Ribeiro, D.V.; Cilla, M.S.; Dias, C.M.R. Accelerated Alkaline Attack of 3D Printing Polymers to Assess Their Durability in Geopolymer-Based Matrices. *J. Mater. Civil. Eng.* **2021**, *33*, 04021327. [CrossRef]
161. Jipa, A.; Reiter, L.; Flatt, R.J.; Dillenburger, B. Environmental Stress Cracking of 3D-Printed Polymers Exposed to Concrete. *Addit. Manuf.* **2022**, *58*, 103026. [CrossRef]
162. Panda, B.; Unluer, C.; Tan, M.J. Extrusion and Rheology Characterization of Geopolymer Nanocomposites Used in 3D Printing. *Compos. B Eng.* **2019**, *176*, 107290. [CrossRef]
163. Zhang, D.-W.; Wang, D.; Lin, X.-Q.; Zhang, T. The Study of the Structure Rebuilding and Yield Stress of 3D Printing Geopolymer Pastes. *Constr. Build. Mater.* **2018**, *184*, 575–580. [CrossRef]
164. Zhou, Z.; Geng, J.; Jin, C.; Liu, G.; Xia, Z. Influence of Residue Soil on the Properties of Fly Ash–Slag-Based Geopolymer Materials for 3D Printing. *Materials* **2024**, *17*, 2992. [CrossRef] [PubMed]
165. Paiva, M.D.M.; Fonseca Rocha, L.D.; Castrillon Fernandez, L.I.; Toledo Filho, R.D.; Silva, E.C.C.M.; Neumann, R.; Mendoza Reales, O.A. Rheological Properties of Metakaolin-Based Geopolymers for Three-Dimensional Printing of Structures. *Mater. J.* **2021**, *118*, 177–187. [CrossRef]
166. Panda, B.; Unluer, C.; Tan, M.J. Investigation of the Rheology and Strength of Geopolymer Mixtures for Extrusion-Based 3D Printing. *Cem. Concr. Compos.* **2018**, *94*, 307–314. [CrossRef]
167. Sando, M.; Stephan, D. The Development of a Fly Ash-Based Geopolymer for Extrusion-Based 3D Printing, along with a Printability Prediction Method. *Case Stud. Constr. Mater.* **2024**, *21*, e03407. [CrossRef]
168. Guo, X.; Yang, J.; Xiong, G. Influence of Supplementary Cementitious Materials on Rheological Properties of 3D Printed Fly Ash Based Geopolymer. *Cem. Concr. Compos.* **2020**, *114*, 103820. [CrossRef]
169. Zhu, X.; Wang, J.; Yang, M.; Xiao, J.; Zhang, Y.; Gilabert, F.A. Performance Modulation and Optimization of PE Fiber Reinforced 3D-Printed Geopolymer. *Constr. Build. Mater.* **2024**, *429*, 136449. [CrossRef]
170. Brandvold, A.S.; Kriven, W.M. Influence of Temperature on Rheological Properties during Early-stage Geopolymerization. *J. Am. Ceram. Soc.* **2024**, *107*, 748–759. [CrossRef]
171. Kashani, A.; Ngo, T.D. Optimisation of Mixture Properties for 3D Printing of Geopolymer Concrete. In Proceedings of the 35th International Symposium on Automation and Robotics in Construction (ISARC 2018), Berlin, Germany, 22–25 July 2018.
172. Rezaei Shahmirzadi, M.; Gholampour, A.; Kashani, A.; Ngo, T.D. Geopolymer Mortars for Use in Construction 3D Printing: Effect of LSS, Graphene Oxide and Nanoclay at Different Environmental Conditions. *Constr. Build. Mater.* **2023**, *409*, 133967. [CrossRef]
173. Lv, X.; Qin, Y.; Liang, H.; Cui, X. Effects of Modifying Agent on Rheology and Workability of Alkali-Activated Slag Paste for 3D Extrusion Forming. *Constr. Build. Mater.* **2021**, *302*, 124062. [CrossRef]
174. Sariyev, B.; Konysbekov, A.; Jexembayeva, A.; Konkanov, M. A Comparative Study of the Rheological Properties of a Fly Ash-Based Geopolymer Reinforced with PP Fiber for 3D Printing: An Experimental and Numerical Approach. *Buildings* **2024**, *14*, 2068. [CrossRef]
175. Chen, Y.; Zhang, L.; Wei, K.; Gao, H.; Liu, Z.; She, Y.; Chen, F.; Gao, H.; Yu, Q. Rheology Control and Shrinkage Mitigation of 3D Printed Geopolymer Concrete Using Nanocellulose and Magnesium Oxide. *Constr. Build. Mater.* **2024**, *429*, 136421. [CrossRef]
176. Saadati, F.; Kani, E.N. Phosphorous Slag-Based Geopolymer Cement Incorporate with Mullite for 3D Printing Application. *Constr. Build. Mater.* **2023**, *406*, 133444. [CrossRef]
177. Brandvold, A.S.; Trindade, A.C.C.; Kriven, W.M. Rheological Assessment of Metakaolin-based Geopolymer Composites through Squeeze Flow. *J. Am. Ceram. Soc.* **2023**, *106*, 4038–4051. [CrossRef]

178. Brandvold, A.S.; Al-Chaar, G.K.; Kriven, W.M. Isolating the Effects of Thixotropy in Geopolymer Pastes. *J. Am. Ceram. Soc.* **2023**, *106*, 2797–2807. [CrossRef]
179. Tramontin Souza, M.; Simão, L.; Guzi de Moraes, E.; Senff, L.; de Castro Pessôa, J.R.; Ribeiro, M.J.; Novaes de Oliveira, A.P. Role of Temperature in 3D Printed Geopolymers: Evaluating Rheology and Buildability. *Mater. Lett.* **2021**, *293*, 129680. [CrossRef]
180. Ma, S.; Fu, S.; Yang, T.; Li, K.; Chen, G.; Dong, Q.; He, P.; Sun, Z.; Duan, X.; Jia, D.; et al. Unveiling the Critical Role of Rheology Modifiers in Additive Manufacturing of Geopolymers and Their Mechanical Properties. *Addit. Manuf.* **2023**, *78*, 103826. [CrossRef]
181. Ramakrishnan, S.; Pasupathy, K.; Mechtcherine, V.; Sanjayan, J. Printhead Mixing of Geopolymer and OPC Slurries for Hybrid Alkali-Activated Cement in 3D Concrete Printing. *Constr. Build. Mater.* **2024**, *430*, 136439. [CrossRef]
182. Rahemipoor, S.; Hasany, M.; Mehrali, M.; Almdal, K.; Ranjbar, N.; Mehrali, M. Phase Change Materials Incorporation into 3D Printed Geopolymer Cement: A Sustainable Approach to Enhance the Comfort and Energy Efficiency of Buildings. *J. Clean. Prod.* **2023**, *417*, 138005. [CrossRef]
183. Ranjbar, N.; Kuenzel, C.; Gundlach, C.; Kempen, P.; Mehrali, M. Halloysite Reinforced 3D-Printable Geopolymers. *Cem. Concr. Compos.* **2023**, *136*, 104894. [CrossRef]
184. Sun, C.; Xiang, J.; Xu, M.; He, Y.; Tong, Z.; Cui, X. 3D Extrusion Free Forming of Geopolymer Composites: Materials Modification and Processing Optimization. *J. Clean. Prod.* **2020**, *258*, 120986. [CrossRef]
185. Nwaki, W.; Eze, E. Rejuvenating the Market for Earth-Based Building Construction Materials in a Developing Economy. *Civil. Sustain. Urban. Eng.* **2022**, *2*, 110–127. [CrossRef]
186. Ventura, A.; Ouellet-Plamondon, C.; Röck, M.; Hecht, T.; Roy, V.; Higuera, P.; Lecompte, T.; Faria, P.; Hamard, E.; Morel, J.C.; et al. Environmental Potential of Earth-Based Building Materials: Key Facts and Issues from a Life Cycle Assessment Perspective. *RILEM State—Art. Rep.* **2022**, *35*, 261–296. [CrossRef]
187. Idrissi Kaitouni, S.; Charai, M.; Es-sakali, N.; Mghazli, M.O.; El Mankibi, M.; Uk-Joo, S.; Ahachad, M.; Brigui, J. Energy and Hygrothermal Performance Investigation and Enhancement of Rammed Earth Buildings in Hot Climates: From Material to Field Measurements. *Energy Build.* **2024**, *315*, 114325. [CrossRef]
188. Tarhan, Y.; Tarhan, İ.H.; Craveiro, F.; Bartolo, H. Building a Sustainable Future: Examining the Impact of Earth-Based Materials on Civil Engineering Development. In *Proceedings of the 3rd International Conference on Water Energy Food and Sustainability (ICoWEFS 2023)*; Springer: Cham, Switzerland, 2024; pp. 581–590. [CrossRef]
189. Gomes, M.I.; Faria, P.; Gonçalves, T.D. Earth-Based Mortars for Repair and Protection of Rammed Earth Walls. Stabilization with Mineral Binders and Fibers. *J. Clean. Prod.* **2018**, *172*, 2401–2414. [CrossRef]
190. Tarhan, Y.; Tarhan, İ.H.; Craveiro, F.; Bártolo, H. Sustainable Materials for Additive Manufacturing: Earth-Based Concrete. In Proceedings of the 1st International Conference on Water Energy Food and Sustainability (ICoWEFS 2021), Leiria, Portugal, 10–12 May 2021; pp. 708–716. [CrossRef]
191. Paula Junior, A.C.; Jacinto, C.; Turco, C.; Fernandes, J.; Teixeira, E.; Mateus, R. Analysis of the Effect of Incorporating Construction and Demolition Waste on the Environmental and Mechanical Performance of Earth-Based Mixtures. *Constr. Build. Mater.* **2022**, *330*, 127244. [CrossRef]
192. Tarhan, Y.; Perrot, A. Reinforcement of 3D Printable Earth-Based Mortar with Natural Textile Material. *Mater. Today Proc.* 2023; *in press*. [CrossRef]
193. Anonymous. (Webpage WASP). 3d Printing Architecture | 3D Printers | WASP. Available online: https://www.3dwasp.com/en/3d-printing-architecture/ (accessed on 16 May 2024).
194. Anonymous. (Webpage IAAC). IAAC and WASP: New 3D Printing Strategies Towards the Realisation of Load-Bearing Earthen Structures—IAAC. Available online: https://iaac.net/iaac-wasp-new-3d-printing-strategies-towards-realisation-load-bearing-earthen-structures/ (accessed on 16 May 2024).
195. Bajpayee, A.; Farahbakhsh, M.; Zakira, U.; Pandey, A.; Ennab, L.A.; Rybkowski, Z.; Dixit, M.K.; Schwab, P.A.; Kalantar, N.; Birgisson, B.; et al. In Situ Resource Utilization and Reconfiguration of Soils Into Construction Materials for the Additive Manufacturing of Buildings. *Front. Mater.* **2020**, *7*, 504591. [CrossRef]
196. Curth, A.; Pearl, N.; Castro-Salazar, A.; Mueller, C.; Sass, L. 3D Printing Earth: Local, Circular Material Processing, Fabrication Methods, and Life Cycle Assessment. *Constr. Build. Mater.* **2024**, *421*, 135714. [CrossRef]
197. Arrieta-Escobar, J.A.; Derrien, D.; Ouvrard, S.; Asadollahi-Yazdi, E.; Hassan, A.; Boly, V.; Tinet, A.J.; Dignac, M.F. 3D Printing: An Emerging Opportunity for Soil Science. *Geoderma* **2020**, *378*, 114588. [CrossRef]
198. Perrot, A.; Rangeard, D.; Courteille, E. 3D Printing of Earth-Based Materials: Processing Aspects. *Constr. Build. Mater.* **2018**, *172*, 670–676. [CrossRef]
199. Gomaa, M.; Jabi, W.; Soebarto, V.; Xie, Y.M. Digital Manufacturing for Earth Construction: A Critical Review. *J. Clean. Prod.* **2022**, *338*, 130630. [CrossRef]
200. Biggerstaff, A.; Lepech, M.; Fuller, G.; Loftus, D. A Shape Stability Model for 3D Printable Biopolymer-Bound Soil Composite. *Constr. Build. Mater.* **2022**, *321*, 126337. [CrossRef]
201. Alqenaee, A.; Memari, A. Experimental Study of 3D Printable Cob Mixtures. *Constr. Build. Mater.* **2022**, *324*, 126574. [CrossRef]

202. Ji, Y.; Poullain, P.; Leklou, N. The Selection and Design of Earthen Materials for 3D Printing. *Constr. Build. Mater.* **2023**, *404*, 133114. [CrossRef]
203. Asaf, O.; Bentur, A.; Larianovsky, P.; Sprecher, A. From Soil to Printed Structures: A Systematic Approach to Designing Clay-Based Materials for 3D Printing in Construction and Architecture. *Constr. Build. Mater.* **2023**, *408*, 133783. [CrossRef]
204. Benzerara, M.; Guihéneuf, S.; Belouettar, R.; Perrot, A. Combined and Synergic Effect of Algerian Natural Fibres and Biopolymers on the Reinforcement of Extruded Raw Earth. *Constr. Build. Mater.* **2021**, *289*, 123211. [CrossRef]
205. Biggerstaff, A.; Fuller, G.; Lepech, M.; Loftus, D. Determining the Yield Stress of a Biopolymer-Bound Soil Composite for Extrusion-Based 3D Printing Applications. *Constr. Build. Mater.* **2021**, *305*, 124730. [CrossRef]
206. Maierdan, Y.; Armistead, S.J.; Mikofsky, R.A.; Huang, Q.; Ben-Alon, L.; Srubar, W.V.; Kawashima, S. Rheology and 3D Printing of Alginate Bio-Stabilized Earth Concrete. *Cem. Concr. Res.* **2024**, *175*, 107380. [CrossRef]
207. Maierdan, Y.; Zhao, D.; Chokshi, P.H.; Garmonina, M.; Kawashima, S. Rheology, 3D Printing, and Particle Interactions of Xanthan Gum-Clay Binder for Earth Concrete. *Cem. Concr. Res.* **2024**, *182*, 107551. [CrossRef]
208. Tarhan, Y.; Tarhan, İ.H.; Jacquet, Y.; Perrot, A. Mechanical Behaviour of 3D Printed and Textile-Reinforced Eco-Friendly Composites. *J. Sustain. Cem. Based Mater.* **2024**, 1–19. [CrossRef]
209. Varun Raj, P.; Surya Teja, P.; Sai Siddhartha, K.; Kalyana Rama, J.S. Housing with Low-Cost Materials and Techniques for a Sustainable Construction in India-A Review. *Mater. Today Proc.* **2021**, *43*, 1850–1855. [CrossRef]
210. El-Mahdy, D.; Gabr, H.S.; Abdelmohsen, S. SaltBlock as a 3D Printed Sustainable Construction Material in Hot Arid Climates. *J. Build. Eng.* **2021**, *43*, 103134. [CrossRef]
211. Silva, G.; Quispe, L.; Kim, S.; Nakamatsu, J.; Aguilar, R. Development of a Stabilized Natural Fiber-Reinforced Earth Composite for Construction Applications Using 3D Printing. *IOP Conf. Ser. Mater. Sci. Eng.* **2019**, *706*, 012015. [CrossRef]
212. Kruger, J.; Cho, S.; Zeranka, S.; Viljoen, C.; van Zijl, G. 3D Concrete Printer Parameter Optimisation for High Rate Digital Construction Avoiding Plastic Collapse. *Compos. B Eng.* **2020**, *183*, 107660. [CrossRef]
213. Rahul, A.V.; Santhanam, M.; Meena, H.; Ghani, Z. 3D Printable Concrete: Mixture Design and Test Methods. *Cem. Concr. Compos.* **2019**, *97*, 13–23. [CrossRef]
214. Hojati, M.; Li, Z.; Memari, A.M.; Park, K.; Zahabi, M.; Nazarian, S.; Duarte, J.P.; Radlińska, A. 3D-Printable Quaternary Cementitious Materials towards Sustainable Development: Mixture Design and Mechanical Properties. *Results Eng.* **2022**, *13*, 100341. [CrossRef]
215. Chen, Y.; Veer, F.; Copuroglu, O.; Schlangen, E. Feasibility of Using Low CO2 Concrete Alternatives in Extrusion-Based 3D Concrete Printing. *RILEM Bookseries* **2019**, *19*, 269–276. [CrossRef]
216. Boscaro, F.; Quadranti, E.; Wangler, T.; Mantellato, S.; Reiter, L.; Flatt, R.J. Eco-Friendly, Set-on-Demand Digital Concrete. *3D Print. Addit. Manuf.* **2022**, *9*, 3–11. [CrossRef] [PubMed]
217. Howard, I.L.; Shannon, J.; Cost, V.T.; Stovall, M. Davis Wade Stadium Expansion and Renovation: Performance of Concrete Produced with Portland-Limestone Cement, Fly Ash, and Slag Cement. *J. Mater. Civil. Eng.* **2015**, *27*, 04015044. [CrossRef]
218. Craveiro, F.; Nazarian, S.; Bartolo, H.; Bartolo, P.J.; Pinto Duarte, J. An Automated System for 3D Printing Functionally Graded Concrete-Based Materials. *Addit. Manuf.* **2020**, *33*, 101146. [CrossRef]
219. Chen, Y.; Chaves Figueiredo, S.; Li, Z.; Chang, Z.; Jansen, K.; Çopuroğlu, O.; Schlangen, E. Improving Printability of Limestone-Calcined Clay-Based Cementitious Materials by Using Viscosity-Modifying Admixture. *Cem. Concr. Res.* **2020**, *132*, 106040. [CrossRef]
220. Karl, D.; Duminy, T.; Lima, P.; Kamutzki, F.; Gili, A.; Zocca, A.; Günster, J.; Gurlo, A. Clay in Situ Resource Utilization with Mars Global Simulant Slurries for Additive Manufacturing and Traditional Shaping of Unfired Green Bodies. *Acta Astronaut.* **2020**, *174*, 241–253. [CrossRef]
221. Xiang, J.; Liu, L.; Cui, X.; He, Y.; Zheng, G.; Shi, C. Effect of Limestone on Rheological, Shrinkage and Mechanical Properties of Alkali—Activated Slag/Fly Ash Grouting Materials. *Constr. Build. Mater.* **2018**, *191*, 1285–1292. [CrossRef]
222. Xia, J.; Yu, B.; Wang, H.; Han, B.; Chen, Y.; Xie, C. Study on Properties and Pore Structure Characteristics of Cement-Based Materials with Limestone Powder. *J. Phys. Conf. Ser.* **2021**, *1904*, 012022. [CrossRef]
223. Dai, X.; Aydin, S.; Yücel Yardimci, M.; Qiang, R.E.N.; Lesage, K.; De Schutter, G. Rheology, Early-Age Hydration and Microstructure of Alkali-Activated GGBFS-Fly Ash-Limestone Mixtures. *Cem. Concr. Compos.* **2021**, *124*, 104244. [CrossRef]
224. Chen, G.Y.; Chen, C.T.; Chang, T.P. Improvement on Engineering Properties and Volumetric Stability of Alkali-Activated Slag-Based Composite Cementitious Material with Rice Husk Ash and Magnesium Oxide. *J. Chin. Inst. Eng.* **2024**, *47*, 179–191. [CrossRef]
225. Bedarf, P.; Dutto, A.; Zanini, M.; Dillenburger, B. Foam 3D Printing for Construction: A Review of Applications, Materials, and Processes. *Autom. Constr.* **2021**, *130*, 103861. [CrossRef]
226. Markin, V.; Sahmenko, G.; Nerella, V.N.; Nather, M.; Mechtcherine, V. Investigations on the Foam Concrete Production Techniques Suitable for 3D-Printing with Foam Concrete. *IOP Conf. Ser. Mater. Sci. Eng.* **2019**, *660*, 012039. [CrossRef]

227. Jin, F.L.; Zhao, M.; Park, M.; Park, S.J. Recent Trends of Foaming in Polymer Processing: A Review. *Polymers* **2019**, *11*, 953. [CrossRef]
228. Falliano, D.; Restuccia, L.; Ferro, G.A.; Gugliandolo, E. Strategies to Increase the Compressive Strength of Ultra-Lightweight Foamed Concrete. *Procedia Struct. Integr.* **2020**, *28*, 1673–1678. [CrossRef]
229. Raj, A.; Sathyan, D.; Mini, K.M. Physical and Functional Characteristics of Foam Concrete: A Review. *Constr. Build. Mater.* **2019**, *221*, 787–799. [CrossRef]
230. Shang, X.; Qu, N.; Li, J. Development and Functional Characteristics of Novel Foam Concrete. *Constr. Build. Mater.* **2022**, *324*, 126666. [CrossRef]
231. Hilal, A.A.; Thom, N.H.; Dawson, A.R. The Use of Additives to Enhance Properties of Pre-Formed Foamed Concrete. *Int. J. Eng. Technol.* **2015**, *7*, 286–293. [CrossRef]
232. Rahul Rollakanti, C.; Siva Rama Prasad, C.V.; Professor, S.; Pavan Kumar, M. Experimental Investigations and Cost Effectiveness of Preformed Foam Cellular Concrete Blocks in Construction Industry. *J. Xi'an Univ. Arch. Technol.* **2020**, *12*, 5010–5019. [CrossRef]
233. Falliano, D.; Gugliandolo, E.; De Domenico, D.; Ricciardi, G. Experimental Investigation on the Mechanical Strength and Thermal Conductivity of Extrudable Foamed Concrete and Preliminary Views on Its Potential Application in 3D Printed Multilayer Insulating Panels. *RILEM Bookseries* **2019**, *19*, 277–286. [CrossRef]
234. Lublasser, E.; Adams, T.; Vollpracht, A.; Brell-Cokcan, S. Robotic Application of Foam Concrete onto Bare Wall Elements—Analysis, Concept and Robotic Experiments. *Autom. Constr.* **2018**, *89*, 299–306. [CrossRef]
235. Amran, Y.H.M.; Farzadnia, N.; Ali, A.A.A. Properties and Applications of Foamed Concrete; a Review. *Constr. Build. Mater.* **2015**, *101*, 990–1005. [CrossRef]
236. Falliano, D.; De Domenico, D.; Ricciardi, G.; Gugliandolo, E. 3D-Printable Lightweight Foamed Concrete and Comparison with Classical Foamed Concrete in Terms of Fresh State Properties and Mechanical Strength. *Constr. Build. Mater.* **2020**, *254*, 119271. [CrossRef]
237. Cho, S.; van Rooyen, A.; Kearsley, E.; van Zijl, G. Foam Stability of 3D Printable Foamed Concrete. *J. Build. Eng.* **2022**, *47*, 103884. [CrossRef]
238. Liu, C.; Xiong, Y.; Chen, Y.; Jia, L.; Ma, L.; Deng, Z.; Wang, Z.; Chen, C.; Banthia, N.; Zhang, Y. Effect of Sulphoaluminate Cement on Fresh and Hardened Properties of 3D Printing Foamed Concrete. *Compos. B Eng.* **2022**, *232*, 109619. [CrossRef]
239. de Carvalho Bello, C.B.; Cecchi, A. Experiments on Natural Fibers: Durability and Mechanical Properties. *Adv. Mater. Process. Technol.* **2017**, *3*, 632–639. [CrossRef]
240. Varela, H.; Barluenga, G.; Sonebi, M. Rheology Characterization of 3D Printing Mortars with Nanoclays and Basalt Fibers. *Mater. Today Proc.* 2023; *in press*. [CrossRef]
241. Wang, W.; Konstantinidis, N.; Austin, S.A.; Buswell, R.A.; Cavalaro, S.; Cecinia, D. Flexural Behaviour of AR-Glass Textile Reinforced 3D Printed Concrete Beams. *RILEM Bookseries* **2020**, *28*, 728–737. [CrossRef]
242. Dörrie, R.; David, M.; Freund, N.; Lowke, D.; Dröder, K.; Kloft, H. In-Process Integration of Reinforcement for Construction Elements During Shotcrete 3D Printing. *Open Conf. Proc.* **2023**, *3*. [CrossRef]
243. Anonymous. (Webpage 3D Print Industry). 'Project MOONRISE' Scientists 3D Print Lunar Regolith-Based Zero Gravity Structures—3D Printing Industry. Available online: https://3dprintingindustry.com/news/project-moonrise-scientists-3d-print-lunar-regolith-based-zero-gravity-structures-182225/ (accessed on 16 May 2024).

Disclaimer/Publisher's Note: The statements, opinions and data contained in all publications are solely those of the individual author(s) and contributor(s) and not of MDPI and/or the editor(s). MDPI and/or the editor(s) disclaim responsibility for any injury to people or property resulting from any ideas, methods, instructions or products referred to in the content.